Journal of Biological Systems

Ebola virus disease dynamics with some preventive measures: a case study of the 2018-2020 Kivu outbreak

A. J. Ouemba Tassé[2] B. Tsanou [1,2,3,*] J. Lubuma[4] Jean Louis Woukeng [2] Francis Signing [2]

[1]*Department of Science, Mathematics and Applied Mathematics, University of Pretoria Private Bag X20, Pretoria 0028, South Africa*

[2]*Department of Mathematics and Computer Science, University of Dschang, P. O. Box 67, Dschang, Cameroon*
berge.tsanou@up.ac.za, bergetsanou@yahoo.fr[†]

[3] *IRD Sorbonne University, UMMISCO, F-93143, Bondy, France*

[4] *School of Computer Science and Applied Mathematics, University of Witwatersrand Johannesburg, South Africa*

Received (Day Mth. Year)
Revised (Day Mth. Year)

Abstract. To fight against Ebola virus disease, several measures have been adopted. Among them, isolation, safe burial and vaccination occupy a prominent place. In this paper, we present a model which takes into account these three control strategies as well as the indirect transmission through a polluted environment. The asymptotic behaviour of our model is achieved. Namely, we determine a threshold value $\mathcal{R}_c^c$ of the control reproduction number $\mathcal{R}_c$, below which the disease is eliminated in the long run. Whenever the value of $\mathcal{R}_c$ ranges from $\mathcal{R}_c^c$ and 1, we prove the existence of a backward bifurcation phenomenon, which corresponds to the case where a locally asymptotically stable positive equilibrium co-exists with the disease-free equilibrium, which is also locally asymptotically stable. The existence of this bifurcation complicates the control of Ebola, since the requirement of $\mathcal{R}_c$ below one, although necessary is no longer sufficient for the elimination of Ebola, more efforts need to be deployed. When the value of $\mathcal{R}_c$ is greater than one, we prove the existence of a unique endemic equilibrium, locally asymptotically stable. That is the disease may persist and become endemic. Numerically, we fit our model to the reported data for the 2018-2020 Kivu Ebola outbreak which occurred in Democratic Republic of Congo. Through the sensitivity analysis of the control reproduction number, we prove that, the transmission rates of infected alive who are outside hospital are the most influential parameters. Numerically we explore the usefulness of isolation, safe burial combined with vaccination and investigate the importance to combine the latter control strategies to the educational campaigns or/and case finding.

Keywords: Ebola, Isolation, Safe burial, Vaccination, Environmental transmission.

[*]Corresponding author
[†]berge.tsanou@up.ac.za

1. Introduction

In December 2013 and August 2018, two deadliest Ebola virus disease (EVD) outbreaks began in Guinea and DRC (Democratic Republic of Congo), respectively. The first one caused the death of more than 11, 000 persons and the second of about 2, 299 persons.[1,2]

EVD symptoms generally include fever, severe headaches, muscle aches, weakness, vomiting, diarrhoea, stomach pains, loss of appetite and at times hemorrhagic bleeding, which can lead to death.[3,4] It is documented that, some EVD infected individuals may present moderate symptoms, while others severe symptoms.[5–8] In fact, the difference in immunological responses may be related to host genetics and/or partial immunity due to previous infection with a related virus. EVD can be transmitted through close contacts with susceptible individuals and bodily fluids such as blood, stools, vomiting, saliva, urine, sperm, maternal milk, of infected ill or dead.[3]

The Ebola-deceased individuals can transmit the disease during mourning or traditional funerals, which include rites and others practices on their corpses.[9] Thus, to impede the transmission by the deceased, the education of people to safe burial has been at the center of all battles against EVD. However, due to the attachment to cultural norms, many people have contracted EVD through manipulation of Ebola-deceased bodies.[10] Moreover, the lack of adequate equipment has caused the infection of many health workers in the Ebola treatment units (ETU) and hospitals. Thus, responding to the EVD spreading by isolating people has not been always perfect.[11,12] Furthermore, up to now, neither treatment nor vaccine is ratified by the World Health Organization (WHO). But, there are two protocol treatments approved by the U. S. Food and Drug Administration (FDA) against EVD.[13] Moreover, an experimental vaccine named rVSV-ZEBOV developed in the course of 2013-2015 outbreak has demonstrated a great efficacy,[14,15] and was used to control the 2018-2020 Kivu EVD outbreak in DRC through ring vaccination.[16–18] More than 223, 000 persons received the vaccine during that Ebola outbreak.[19] Therefore, the public health officials and the scientific community should consider the combination of vaccination and former control strategies such as isolation and safe burial in the fight against EVD.[16] Such a battle gives floor to a multi-disciplinary research activity among which, mathematical modelling is concerned.

Essentially, mathematical models may help the medical community and decision makers to evaluate the effectiveness of different approaches for bringing an epidemic under control.[20] In this regard, since 2014, many models for EVD focused on control strategies such as contact tracing, isolation, safe burial and vaccination.

For instance, in,[21] the authors proposed a model which includes vaccination and heterogeneity of the risk of becoming infected with EVD. Contrarily to,[21] in,[22] the authors proposed an EVD model with isolation, where the Ebola-deceased individuals are divided in two compartments: those who can transmit the disease and those who can not transmit it, since they are safely buried. They computed the ba-

sic reproduction number and evaluated the efficiency of different control strategies to reduce its value. But, it seems confusing to separate the compartment of hospitalized individuals from that of isolated, since infected people in both classes are settled in a treatment center (which are not opened to the general public[23]). Furthermore, in[24] the authors investigated the usefulness of quarantine and isolation to mitigate EVD outbreaks. They showed numerically that, a good implementation of quarantine and the reduction of contacts between quarantined and infectious individuals can extensively reduce the level of the disease and may eliminate it. However, in their work, the authors assumed that the recovery rate of infected individuals is the same whether they are in hospitals or not. This may be not always the case, and we believe that, this assumption should be relaxed. Beside, in,[25,26] the authors proposed models with vaccination and isolation, where in their first paper, isolated individuals can transmit the disease but in a lesser rate compared to infected non-isolated individuals. They computed the basic reproduction number and performed the sensitivity analysis of the model. Their analysis suggested that, the efficacy of isolation and the time from death to burial have the most influence on the basic reproduction number than all others parameters. In their second paper, the same authors assessed the efficiency of vaccination and quarantine in the fight against EVD. The modelling concern we have about[25] is the fact that, the authors assumed that, the latent and symptomatic individuals are isolated and gathered in the same epidemiological compartment, knowing that EVD is unlikely be transmitted during the incubation period. The authors in[27] proposed a model with a fear-dependent transmission rate. They showed the existence of a forward and a backward bifurcations and numerically determined the direction of these bifurcations. Moreover, they fitted their model to the reported data for the 2018-2020 Kivu EVD outbreak and proved the decrease of the number of infected individuals as the level of fear due to EVD increases. In the other hand, in,[26] the authors did not take into account the infectivity potential of Ebola-deceased individuals. The same drawbacks can equally be highlighted in the models with isolation proposed in.[28–32] In,[6] the authors proposed an innovative model with isolation which takes into account the transmissibility of individuals with moderate symptoms, severe symptoms and Ebola-deceased. However, they neglected the fact that, some infected may progress from moderate symptoms to severe symptoms,[33] and the transmission through the environment. Moreover, it is not clearly explained/motivated why individuals with moderate symptoms can not recover.

In this paper, we focus on the above mentioned three main prevention strategies which are: vaccination, imperfect isolation and safe burial by combining them in a single model, with the aims to fill many (if not all) of the drawbacks highlighted the above-mentioned papers. However, one should not lose sight that, contact tracing is another efficient control measure for Ebola which has already been investigated by us and other authors.[34,35] Our propounded model is qualitatively and quantitatively analyzed. Qualitatively, we prove the existence of a threshold value $\mathcal{R}_c^c$ of the control reproduction number $\mathcal{R}_c$, below which the disease-free equilibrium (DFE)

is globally asymptotically stable (GAS), that is EVD is eliminated. Whenever the value of $\mathcal{R}_c$ is between $\mathcal{R}_c^c$ and 1, we prove the existence of a backward bifurcation. While, when the value of $\mathcal{R}_c$ is greater than one, we show that our model admits a unique endemic equilibrium, locally asymptotically stable (LAS). That is the disease may persist and can be endemic. Quantitatively, we fit our model to the real data for the 2018-2020 Kivu EVD outbreak. Through the sensitivity analysis, we derive the most influential parameters at the beginning of the outbreak. Furthermore, we investigate numerically the impact of the transmission through the environment, the efficacy of the isolation, safe burial and vaccination, and the usefulness to combine these control strategies with the case finding and the educational campaigns (not initially addressed by our model). We stress that, the initial idea of this work started with a preprint[36] titled differently, yet not fully developed to incorporate the environmental transmission and to estimate model parameters of our model. Thus, the two manuscripts share some similitude in their introduction and model formulation parts.

The rest of this paper is organized as follows. In Section 2, the model is built in a comprehensive manner and a corresponding system of ordinary differential equations is derived. The asymptotic behaviour of the model is provided in Section 3, through the global asymptotic stability of the disease-free equilibrium (DFE) and the local stability of the endemic equilibrium. The local sensitivity analysis of the control reproduction number is presented in Section 4. Numerical simulations are used to investigate different isolated and combination of control strategies in Section 5, and the discussion and perspectives are provided in Section 6.

2. Model formulation

2.1. *Main assumptions*

1. The isolation is not always effective. Moreover hospitals and Ebola Treatment Unit (ETUs) are isolation settings.
2. Some EVD infected individuals who succumb to EVD are safely buried by well-trained personal, when their family members are educated accordingly.
3. The asymptomatic infected individuals do not transmit EVD (even though there is evidence of asymptomatic carriers,[37] the very low level of virus detected in them do not indicate a significant source of transmission[38,39]).

2.2. *Model variables*

Our population is subdivided into the following mutually exclusive classes:

- $S(t)$: Individuals at risk of becoming infected i.e the susceptible individuals.
- $J(t)$: Infected individuals with moderate symptoms who are outside hospitals/ETUs. We recall that those symptoms include fever, sore throat, muscular pain and headaches.[40]

- $I(t)$: Infected individuals with severe symptoms (i.e vomiting, bloody diarrhoea and rash) who are outside hospitals/ETUs.[3,4,40]
- $H(t)$: Infected individuals who are under treatment (in hospitals/ETUs). We call them interchangeably isolated or hospitalized individuals.
- $D(t)$: Dead bodies of Ebola infected individuals who did not survive (did not recover). This is actually an infectious class which gathers all the Ebola infected individuals who die inside and outside hospitals/ETUs. The rationale of considering this class is the fact that, it is well documented that Ebola-deceased individuals are infectious if not properly handled.[34,41]
- $R(t)$: Recovered individuals. Even though, up to now, there is no available treatment for EVD, some patients have recovered after receiving supportive treatments,[42] but the chances of surviving decrease as the symptoms increase (thus, the recovery rate in compartment J is greater than the one of the compartment I). Moreover, since it is documented that recovered individuals develop antibodies that last for at least 10 years,[34,43] we assume that they are permanently immune.
- $V(t)$: Concentration of the Ebola viruses in the environment at unit time t. This class is replenished by the Ebola viruses shed by infected alive or dead. The introduction of this compartment is motivated by the persistence of the Ebola virus in the environment, through which some individuals contract the infection (see for instance[44] and references therein).

Let $N(t)$ denote the total human population including dead individuals. That is:

$$N(t) = S(t) + J(t) + I(t) + H(t) + D(t) + R(t). \tag{2.1}$$

Remark 2.1 *Despite the fact that, individuals of the compartment J can caused more contacts with susceptible individuals than those of compartment I, it is well known that, the infectivity of Ebola virus disease patients increases as the disease symptoms increase. Furthermore, Ebola-deceased individuals are highly contagious than alive infected.[45] However, under isolation the contact rate between susceptible and isolated individuals is minimal. Thus, though the infectivity of isolated individuals increases with disease symptoms, their effective transmission rate is less than those of the compartments J and I.[41]*

2.3. *Derivation of model equations*

Susceptible individuals in S are recruited at a constant rate π by immigration/births, and vaccinated at rate τ. Among vaccinated individuals, a proportion θ acquires immunity (since no vaccine is 100% effective[46]). The other susceptible individuals can be infected (i)-through contact with individuals in J and I classes at rates β and $\beta\nu_1$ respectively, (ii)-through contact with $(1-\sigma_1)H$ individuals who are not effectively isolated (where σ_1 represents the proportion of infected who are effectively isolated) at rate $\varepsilon\beta$, (iii)-through contact with $(1-\sigma_2)D$ Ebola-deceased

individuals who failed safe burial (where σ_2 is the proportion of Ebola-deceased individuals safely buried) at rate $\beta\nu_2$, or (iv) through contact with a contaminated environment, at rate β_v. Since human immune system reacts differently, a proportion p of infected individuals may present moderate symptoms while the remaining proportion exhibits severe symptoms. The individuals in class J can recover (without being in at hospital/ETU) at rate γ_j; die due to the disease at rate δ_j; go to the hospital at rate η_j or progress to compartment I at rate α.[33] Those in compartment I can pass away due to EVD at rate δ_i, be hospitalized at rate η_i or can recover at rate γ_i (with $\gamma_i \leq \gamma_j$), by any other means than medical treatment. Hospitalized individuals recover at rate γ_h or die due to EVD at rate δ_h. The uninfected population is affected by the natural mortality rate μ, with $\mu \leq \min\{\delta_j, \delta_i, \delta_h\}$. Infected in compartments J, I, H and D shed viruses in the environment at rates q_1, q_2, q_3 and q_4 respectively, but these viruses deplete naturally or through environmental decontamination techniques at a constant rate u.

Let

$$\lambda(t) = \frac{\beta\left(J + \varepsilon(1-\sigma_1)H + \nu_1 I + \nu_2(1-\sigma_2)D\right)}{N} + \beta_v V$$

The model parameters and their biological meanings are summarized in Table 1, the transmission diagram of the disease is displayed in Figure 1, and the resulted system of ordinary differential equations is as follows:

$$\begin{cases} \dot{S}(t) &= \pi - \lambda S - (\tau\theta + \mu)S, \\ \dot{J}(t) &= p\lambda S - (\alpha + \gamma_j + \delta_j + \eta_j)J, \\ \dot{I}(t) &= (1-p)\lambda S + \alpha J - (\delta_i + \eta_i)I, \\ \dot{H}(t) &= \eta_j J + \eta_i I - (\delta_h + \gamma_h)H, \\ \dot{D}(t) &= \delta_j J + \delta_i I + \delta_h H - bD, \\ \dot{R}(t) &= \tau\theta S + \gamma_j J + \gamma_i I + \gamma_h H - \mu R, \\ \dot{V}(t) &= q_1 J + q_2 I + q_3 H + q_4 D - uV. \end{cases} \tag{2.3}$$

In order to simplify the notations and avoid lengthy expressions, we define the parameters:

$$\begin{array}{llll} \sigma_h = \varepsilon(1-\sigma_1), & \sigma_d = \nu_2(1-\sigma_2), & \theta_1 = \theta\tau, & \theta_2 = \mu + \theta\tau, \\ \phi_1 = (\alpha + \delta_j + \gamma_j + \eta_j), & & \phi_2 = (\delta_i + \eta_i), & \phi_3 = (\gamma_h + \delta_h), \end{array}$$

Thus, Model (2.3) becomes

$$\begin{cases} \dot{S}(t) &= \pi - \lambda S - \theta_2 S, \\ \dot{J}(t) &= p\lambda S - \phi_1 J, \\ \dot{I}(t) &= (1-p)\lambda S + \alpha J - \phi_2 I, \\ \dot{H}(t) &= \eta_j J + \eta_i I - \phi_3 H, \\ \dot{D}(t) &= \delta_j J + \delta_i I + \delta_h H - bD, \\ \dot{R}(t) &= \theta_1 S + \gamma_j J + \gamma_i I + \gamma_h H - \mu R, \\ \dot{V}(t) &= q_1 J + q_2 I + q_3 H + q_4 D - uV. \end{cases} \tag{2.4}$$

The mathematical proofs of our theoretical results are provided in the Appendix so that the interested reader is refereed to it for details.

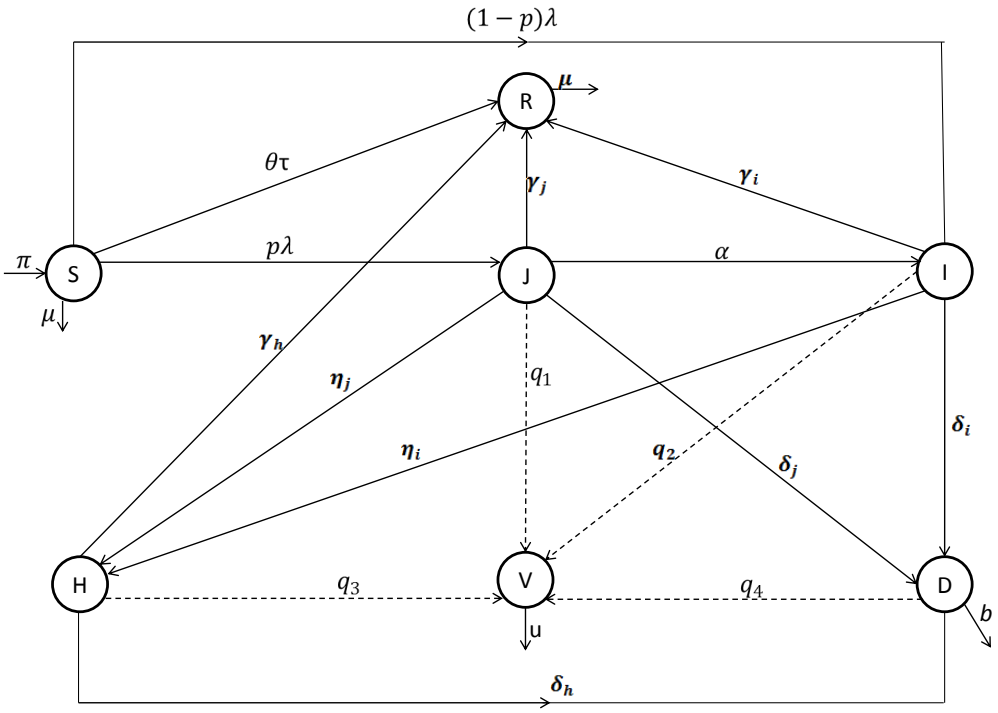

Fig. 1. Transmission diagram of the model

3. Analytical results

3.1. *Well-posedness of model* (2.3)

Proposition 3.1 *The positively orthant* $\mathbb{R}^7_+$ *is positively invariant under the flow of* (2.3). *Namely, if*

$$S(0) > 0, J(0) \geq 0, I(0) \geq 0, H(0) \geq 0, D(0) \geq 0, R(0) \geq 0, V(0) \geq 0,$$

then for all $t > 0$,

$$S(t) > 0, J(t) \geq 0, I(t) \geq 0, H(t) \geq 0, D(t) \geq 0, R(t) \geq 0, V(t) \geq 0.$$

Proposition 3.2 *Let's denote*

$$M(t) = S(t) + J(t) + I(t) + H(t) + R(t), \forall\, t \geq 0.$$
$$\Lambda_1 = \frac{b\pi(q_1+q_2+q_3) + q_4\pi(\delta_j+\delta_i+\delta_h)}{ub(\mu+\delta_j+\delta_i+\delta_h)}$$
$$\Lambda_2 = \frac{b\pi(q_1+q_2+q_3) + q_4\pi(\delta_j+\delta_i+\delta_h)}{ub\mu}.$$

Table 1. Parameters and epidemiological interpretation of Model (2.3).

Parameter	Epidemiological interpretation	units
π	Number of susceptible individuals recruited.	$indiv.week^{-1}$
μ	Natural mortality rate.	$week^{-1}$
p	Proportion of infected with moderate symptoms.	-
τ	Vaccination rate.	$week^{-1}$
θ	Proportion of vaccinated individuals with livelong immunity.	-
β	Effective transmission rate of individuals in compartment J.	$indiv.week^{-1}$
β_v	Effective transmission rate through the polluted environment.	$week^{-1}$
ν_1	Modification parameter for the transmission of individuals with severe symptoms.	-
ν_2	Modification parameter for the transmission of the Ebola-deceased individuals.	-
ε	Modification parameter for the transmission of hospitalized individuals.	
σ_1	Proportion of hospitalized individuals who are effectively isolated.	-
σ_2	Proportion of safely burial Ebola-deceased individuals.	-
η_j	Hospitalization rate of individuals in compartment J.	$week^{-1}$
η_i	Hospitalization rate of individuals in compartment I.	$week^{-1}$
δ_i	Mortality rate due to EVD in compartment I.	$week^{-1}$
δ_j	Mortality rate due to EVD in compartment J.	$week^{-1}$
δ_h	Mortality rate due to EVD in compartment H.	$week^{-1}$
γ_j	Recovery rate in compartment J.	$week^{-1}$
γ_i	Recovery rate in compartment I.	$week^{-1}$
γ_h	Recovery rate in compartment H.	$week^{-1}$
α	Proportion of individuals in compartment J who progress to the I-compartment.	$week^{-1}$
b	Burial rate of Ebola-deceased individuals.	$week^{-1}$
u	Decay rate of viruses in the environment.	$week^{-1}$
q_1	Deposition/shedding rate of viruses in the environment by infected of compartment J[47]	$cells.(ml.week.indiv)^{-1}$
q_2	Deposition/shedding rate of viruses in the environment by infected of compartment I.	$cells.(ml.week.indiv)^{-1}$
q_3	Deposition/shedding rate of viruses in the environment by infected of compartment H.	$cells.(ml.week.indiv)^{-1}$
q_4	Deposition/shedding rate of viruses in the environment by infected of compartment D.	$cells.(ml.week.indiv)^{-1}$

The Model (2.3) *is a dynamical system on*

$$\Omega := \left\{ (S(t), J(t), I(t), H(t), D(t), V(t)) \in \mathbb{R}_+^7 / \frac{\pi}{(\mu + \delta_j + \delta_i + \delta_h)} \leq M(t) \leq \frac{\pi}{\mu}, \right.$$
$$\left. , \frac{\pi(\delta_j + \delta_i + \delta_h)}{b(\mu + \delta_j + \delta_i + \delta_h)} \leq D(t) \leq \frac{\pi(\delta_j + \delta_i + \delta_h)}{b\mu} \text{ and } \Lambda_1 \leq V(t) \leq \Lambda_2 \right\},$$

which is positively invariant and absorbing with respect to the flow of System (2.3).

3.2. *Equilibria of Model* (2.3)

For simplicity, we adopt the following notations.

$$\begin{cases} k_1 = \eta_j\phi_2 + \eta_i\alpha, \quad k_2 = p\alpha + \phi_1(1-p), \quad k_3 = pk_1 + (1-p)\phi_1\eta_i, \\ k_4 = \delta_j p\phi_2\phi_3 + \delta_i k_2\phi_3 + \delta_h k_3, \quad k_5 = \gamma_j p\phi_2\phi_3 + \gamma_i k_2\phi_3 + \gamma_h k_3, \\ k_6 = pb\phi_2\phi_3\mu + k_2\phi_3 b\mu + k_3 b\mu + k_4\mu + k_5 b, \\ k_7 = q_1 pb\phi_2\phi_3 + q_2 k_2\phi_3 b + q_3 k_3 b + q_4 k_4, \quad A_2 = \pi ubk_6\phi_1\phi_2\phi_3, \\ A_1 = u\pi b^2\phi_1^2\phi_2^2\phi_3^2\theta_2 + \pi k_6\theta_2 ub\phi_1\phi_2\phi_3 - \beta_v\pi^2 k_7 k_6 \\ \qquad -\beta\pi\mu ub\phi_1\phi_2\phi_3(pb\phi_2\phi_3 + \nu_1 k_2\phi_3 b + \sigma_h k_3 b + \sigma_d k_4) \\ A_0 = \theta_2^2 ub^2\phi_1^2\phi_2^2\phi_3^2\pi - \theta_2\beta\pi\mu ub\phi_1\phi_2\phi_3(p\phi_2\phi_3 b + \nu_1 k_2\phi_3 b + \sigma_h k_3 b + \sigma_d k_4) \\ \qquad -\phi_1\phi_2\phi_3\pi^2 b\beta_v k_7\theta_2. \end{cases} \tag{3.1}$$

A_0 can be written such as

$$A_0 = \pi b^2\theta_2^2 u\phi_1^2\phi_2^2\phi_3^2(1-\mathcal{R}_c),$$

with

$$\mathcal{R}_c = \frac{\beta\mu(p\phi_2\phi_3 b + \nu_1 k_2\phi_3 b + \sigma_h k_3 b + \sigma_d k_4)}{b\theta_2\phi_1\phi_2\phi_3} + \frac{\beta_v k_7\pi}{bu\theta_2\phi_1\phi_2\phi_3}.$$

Furthermore, let's denote

$$\mathcal{R}_c^c = 1 - \frac{A_1^2}{4A_2\pi b^2 u\theta_2^2\phi_1^2\phi_2^2\phi_3^2}.$$

The existence of the equilibria for the Model (2.3) are discussed in the theorem below, whose proof is given in Appendix B.

Theorem 3.1

- *If $\mathcal{R}_c \leq \mathcal{R}_c^c$, then the Model* (2.3) *admits a unique equilibrium: the disease-free equilibrium (DFE) E_0, $E_0 = (S_0, 0, 0, 0, 0, R_0, 0)$ with $S_0 = \dfrac{\pi}{\theta_2}$, $R_0 = \dfrac{\pi\theta_1}{\mu\theta_2}$.*
- *If $\mathcal{R}_c^c \leq \mathcal{R}_c < 1$, then the Model* (2.3) *has three equilibria: the DFE and two positive equilibria.*
- *If $\mathcal{R}_c > 1$, then our model admits exactly two equilibria: the DFE and a unique endemic equilibrium (which will be denoted by E_1).*

3.3. *Bifurcation analysis*

The proof of the Theorem 3.1 in Appendix B shows that, the existence of positive equilibria for Model (2.3) when $\mathcal{R}_0^c \leq \mathcal{R}_c < 1$ is discussed through the roots of the equation

$$A_2\lambda^{*2} + A_1\lambda^* + A_0 = 0.$$

Thus, let's define the function $G(\beta;\lambda^*)$ by:

$$G(\beta;\lambda^*) := A_2\lambda^{*2} + (B_1 - \beta B_2)\lambda^* + C_1 - \beta C_2 = 0. \tag{3.3}$$

with

$$B_1 = u\pi b^2\phi_1^2\phi_2^2\phi_3^2\theta_2 + \pi k_6\theta_2 ub\phi_1\phi_2\phi_3,$$
$$B_2 = \pi\mu ub\phi_1\phi_2\phi_3(pb\phi_2\phi_3 + \nu_1 k_2\phi_3 b + \sigma_h k_3 b + \sigma_d k_4) + \sigma_v\pi^2 k_7 k_6,$$
$$C_1 = \theta_2^2 ub^2\phi_1^2\phi_2^2\phi_3^2\pi,$$
$$C_2 = \theta_2\pi\mu ub\phi_1\phi_2\phi_3(p\phi_2\phi_3 b + \nu_1 k_2\phi_3 b + \sigma_h k_3 b + \sigma_d k_4) + \phi_1\phi_2\phi_3\pi^2 b\sigma_v k_7\theta_2.$$

Note that, the above parameters are linked by the following relations

$$A_1 = B_1 - \beta B_2, \quad A_0 = C_1 - \beta C_2, \text{ with } \sigma_v := \frac{\beta_v}{\beta}.$$

We focus in the solutions λ^* for a given value of β. For $\lambda^* = 0$, one has

$$\beta^{**} = \frac{C_1}{C_2} = \frac{1}{\mathcal{R}_c}.$$

We compute the bifurcation direction afterwards, defined by:

$$\frac{d\lambda^*}{d\beta^{**}} = -\frac{G_{\beta^{**}}}{G_{\lambda^*}}, \text{ with } G_{\beta^{**}}(\beta^{**}, 0) = -B_2\lambda^* - C_2, G_{\lambda^*}(\beta^{**}, 0) = 2A_2\lambda^* + B_1 - \beta^{**}B_2.$$

and

$$G_{\beta^{**}}(\beta^{**}, 0) = -C_2 < 0, \quad G_{\lambda^*}(\beta^{**}, 0) = B_1 - \beta^{**}B_2.$$

Thus,

$$G_{\lambda^*}(\beta^{**}, 0) < 0 \Leftrightarrow \mathcal{R}_c < \frac{B_2}{B_1}.$$

Hence, if $\mathcal{R}_c < \frac{B_2}{B_1}$, then the bifurcation is backward and if $\mathcal{R}_c > \frac{B_2}{B_1}$, the bifurcation is forward.

Let's recall that, the bifurcation is a change of the topological structure of a system when its parameters pass through a critical value.[27] The biological consequence of a backward bifurcation, is that, the requirement $\mathcal{R}_c < 1$, although necessary is no longer sufficient for a global elimination of EVD.[23] Thus, the existence of a backward bifurcation makes the effective control of EVD difficult, since the value of $\mathcal{R}_c$ need to be less than its critical value $\mathcal{R}_c^c$. Figure 2(a) gives an example of the construction of the backward bifurcation. We observe that a locally asymptotically stable (LAS) DFE co-exists with a LAS endemic equilibrium (EE) when the value of $\mathcal{R}_c$ is greater than $\mathcal{R}_c^c$ and less than one. The Figure 2(b) gives an example of a construction of a forward bifurcation, which means that the disease will persist in the community for a value of $\mathcal{R}_c$ greater than one.

Remark 3.1 *$\mathcal{R}_c$ defined above is the control reproduction number for Model* (2.3)*. That is the number of secondary infections, produced by one infectious, introduced in a completely susceptible population during its entire infectious period, despite the implementation of the vaccination, the isolation and the safe burial. Moreover, $\mathcal{R}_c$ can be decomposed in the following form*

$$\mathcal{R}_c = \mathcal{R}_h + \mathcal{R}_v,$$

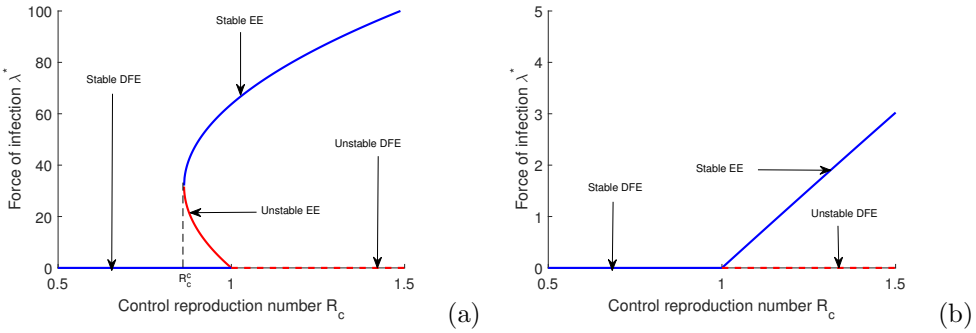

Fig. 2. Figure (a): Backward bifurcation for $\beta = 0.1130, \mu = 6.1, \nu_1 = 14.67, v = 2.005, \varepsilon = 0.08, b = 0.00001, \gamma_h = 1000.19366, \delta_h = 0.00029, \alpha = 10.25, u = 50.22, \gamma_1 = 0.33$ and Figure (b): Forward bifurcation for $\mu = 14.10, \beta = 0.1130, v = 2.005, \varepsilon = 0.08, b = 1/2.01, \gamma_h = 0.19366, \gamma_i = 0.33$. (The other parameters are in Table 2).

where

$$\mathcal{R}_h = \frac{\beta\mu(p\phi_2\phi_3 b + \nu_1 k_2\phi_3 b + \sigma_h k_3 b + \sigma_d k_4)}{b\theta_2\phi_1\phi_2\phi_3} \quad \text{and} \quad \mathcal{R}_v = \frac{\beta_v k_7 \pi}{bu\theta_2\phi_1\phi_2\phi_3},$$

are respectively the contributions of the infections through direct contacts and indirect contacts, to the control reproduction number. Indirect transmission of EVD refers to the transmission through contacts with the viruses shed in the environment, while direct transmission stands for the transmission through contacts with infected individuals in classes J, I, H and D. Furthermore, with the latter in mind, the expression of $\mathcal{R}_h$ can be also written as:

$$\mathcal{R}_h = \mathcal{R}^J + \mathcal{R}^I + \mathcal{R}^I + \mathcal{R}^H + \mathcal{R}^D,$$

with

$$\mathcal{R}^J = \frac{p\beta\mu}{\phi_1\theta_2}, \qquad \mathcal{R}^I = \frac{\beta\nu_1\mu k_2}{\theta_2\phi_1\phi_2}$$

$$\mathcal{R}^H = \frac{\beta\sigma_h\mu k_3}{\phi_1\phi_2\phi_3\theta_2}, \mathcal{R}^D = \frac{\beta\sigma_d\mu k_4}{b\theta_2\phi_1\phi_2\phi_3},$$

are the contributions of infected with moderate symptoms, severe symptoms, hospitalized individuals, and deceased who have been formerly infected by the Ebola virus, respectively.

The relevance of the control reproduction number with regard to the elimination of EVD is investigated in the following paragraph.

3.4. *Global stability of the disease-free equilibrium*

Theorem 3.2 *If the control reproduction number $\mathcal{R}_c$ is less than $\mathcal{R}_c^c$, then the DFE E_0 of Model (2.3) is GAS and it is unstable when $\mathcal{R}_c > 1$.*

The biological interpretation of the following result is that, EVD can be globally eliminated if the control reproduction number $\mathcal{R}_c$ is less than one.

We have proven the existence of a unique endemic equilibrium if the control reproduction number $\mathcal{R}_c$ is greater than one. It is therefore important to investigate its stability, which unfortunately implies that, in this case, the disease cannot be eliminated if additional mitigated actions are taken. This is mathematically stated in the next result and proved in Appendix D.

3.5. *Local stability of the endemic equilibrium*

Theorem 3.3 *If $\mathcal{R}_c > 1$, then System (2.3) undergoes a trans-critical bifurcation with $\mathcal{R}_c = 1$ being the bifurcation parameter. Moreover, the unique endemic equilibrium E_1 is LAS.*

4. Sensitivity analysis of the control reproduction number

The sensitivity analysis is important in designing the control strategies that can be chosen at the onset of EVD outbreak, since it may help us to identify among parameters those which are most influential. In order to see how a small perturbation made to a parameter q affects the control reproduction number $\mathcal{R}_c$, we define the forward normalized sensitivity index of $\mathcal{R}_c$ for q as follows:[34]

$$\epsilon_q^{\mathcal{R}_c} = \frac{\partial \mathcal{R}_c}{\partial q} . \frac{q}{\mathcal{R}_c}.$$

The sensitivity indices of $\mathcal{R}_c$ for our parameters are computed and their values displayed in Table 2.

It is well known that, $\epsilon_q^{\mathcal{R}_c}$ is positive if $\mathcal{R}_c$ is increasing with respect to q and negative if $\mathcal{R}_c$ is decreasing with respect to q.[34] Namely, the fact that $\epsilon_\pi^{\mathcal{R}_c} = 0.0023$ means that, if we increase 1% in π, keeping the other parameters fixed, will produce 0.0023% increase in $\mathcal{R}_c$.[48] Similarly, $\epsilon_\tau^{\mathcal{R}_c} = -0.2725$ means increasing the parameter τ of 1%, keeping the value of the other parameters fixed, the value of $\mathcal{R}_c$ will decrease of 0.2725%. Following Table 2, β and ν_1 are the most influential parameters that can contribute to the increase of the value of $\mathcal{R}_c$; while $\delta_i, \sigma_2, \theta, \tau$ are the most influential which contribute to its reduction. The impact of the parameters β_1 and ν_1 on the value of $\mathcal{R}_c$ add credit to the fact that reducing contacts early between suspected and infected individuals can bring down the size of $\mathcal{R}_c$ to a value less than one.[6,41,49] Moreover, the usefulness of the parameters δ_i and τ to reduce the control reproduction number and the size of EVD outbreaks would have been predicted by the works[34,50] and,[21,51] respectively.

The results obtained in the sensitivity analysis suggest that, it is useful to address the educational campaigns[49] or/and the case finding in order to mitigate the negative impact of the parameters β and ν_1. Indeed through the educational campaigns, the susceptible individuals will be able to recognize probable infected cases and will avoid contact with them; while the case finding may help to isolate some

infected with the aim of cutting the chain of transmission. Moreover, this analysis highlights that, at the beginning of EVD, safe burial of Ebola deceased individuals lead to less number of infected than vaccination does.

5. Numerical simulations

In this paragraph, we carried out few simulations in order to estimate model parameters and to explore the importance of control strategies (isolation, safe burial, vaccination) implemented in Model (2.3) against EVD as well as other additional measures such as the case finding or the educational campaigns.

5.1. *Model validation for the 2018-2020 Kivu EVD outbreak*

Some parameters of Model (2.3) are found in the literature (as indicated in Table 2). The other parameters such as the parameter p, the death rates or the recovery rates can vary from one outbreak to another. To estimate these parameters, we fit in Figure 3 our model to the weekly reported cases during the 2018-2020 Kivu EVD outbreak,[27] using the Nonlinear Least Squares method, which allows the determination of the set of parameters that minimizes the sum of the squares of the differences between the cumulative number of infected predicted by the Model (2.3) and the observed cumulative infected. To plot the fitting curve generated by Model (2.3) we estimate the population of North kivu and South kivu at about 11, 000, 000 of people.[52,53] Moreover, we choose the initial conditions: $S(0) = 11,\,000,\,000; J(0) = 300; I(0) = 300; H(0) = 300; D(0) = 400; R(0) = 200; V(0) = 5$. The obtained parameters are reported in Table 2.

In order to assess the accuracy of our predictions, we calculate two performance metrics: The Mean Absolute Error (MAE) and the Root Mean Square Error (RMSE), which are defined as follows:[48]

$$MAE = \frac{1}{N_p}\sum_{i=1}^{N_p}|Y(i) - \hat{Y}(i)|$$

$$RMSE = \sqrt{\frac{\sum_{i=1}^{N_p}(Y(i) - \hat{Y}(i))^2}{N_p}},$$

where $Y(i)$ represent original cases, $\hat{Y}(i)$ are predicted values and N_p is the size of the data. The computation of these metrics gives: $MAE = 0.1809$ and $RMSE = 1.3539$. These weak values of MAE and RMSE prove that our model performs excellently the case of the 2018-2020 Kivu EVD outbreak. Figure 3 shows that, our model is a very good fit of the cumulative real cases during the 2018-2020 Kivu EVD outbreak, and can then be used to predict the course of EVD outbreaks.

Remark 5.1 *Note that, with the parameters values estimated for the 2018-2020 Kivu EVD outbreak, the value of the control reproduction number* $\mathcal{R}_c = 0.33$*, with*

Table 2. Parameters values for Model (2.3).

Parameters	Values.weeks^{-1}	References	Sensitivity index
π	400	[3]	0.0023
p	0.5708	Fitted	0.107
τ	0.005	[50]	-0.2725
θ	0.9	[54]	-0.288
β	0.16	[55]	0.994
ν_1	1.5267	Fitted	0.627
ν_2	1.5	[10]	0.148
ε	0.3875	[34]	0.05859
γ_j	0.3796	Fitted	-0.159
σ_1	0.3074	Fitted	-0.026
σ_2	0.7086	Fitted	-0.359
η_j	0.2311	Fitted	-0.0433
μ	10.13/1000	[34]	0.3531
η_i	0.25	[34]	-0.2128
δ_i	0.3079	Fitted	-0.436
δ_j	0.0152	Fitted	-0.0014
δ_h	0.1808	Fitted	0.0082
γ_h	0.4594	Fitted	0.082
γ_i	0.0153	Fitted	-0.0217
α	0.5723	Fitted	-0.1413
b	1/2.01	[10]	-0.149
u	0.4019	Fitted	0.0023
q_1	0.05	[27]	0.00024
q_2	0.05	[27]	0.0006
q_3	0.1173	Fitted	0.0008
q_4	0.06	[27]	0.0012
β_v	5.07×10^{-8}	[56]	0.0023

the contributions of infected of compartments J, I, H, D and V to the control reproduction number equal to: $\mathcal{R}_c^J = 0.0528$; $\mathcal{R}_c^I = 0.2071$; $\mathcal{R}_c^H = 0.0193$; $\mathcal{R}_c^D = 0.0488$ *and* $\mathcal{R}_v = 7.6507 \times 10^{-4}$*, respectively. This relatively low value of the control reproduction number may be due to the great experience DRC has in the fighting against EVD, knowing that the country had faced many outbreaks and has developed efficient means to protect its population. For instance, without the account of vaccination in our model (that is for $\tau = 0$), the control reproduction number were be equal to 0.48, which is near to 0.51, obtained after intervention in DRC in 1995.*[57] *Moreover, the $\mathcal{R}_c$ contributed values estimated by $\mathcal{R}_c^J, \mathcal{R}_c^I, \mathcal{R}_c^H, \mathcal{R}_c^D$ and $\mathcal{R}_c^V$ suggest that, to rapidly eliminate EVD in DRC, one should address control measures which target the infected showing severe symptoms (because, among the five contributions, that of $\mathcal{R}_c^I$ alone represents about $0.2071/0.33 = 62\%$ of the value of $\mathcal{R}_c$). However, in the course of EVD, one shall show that the outcomes (model variables) are very sensitive to the disease transmission rate (β_v) through the environment.*

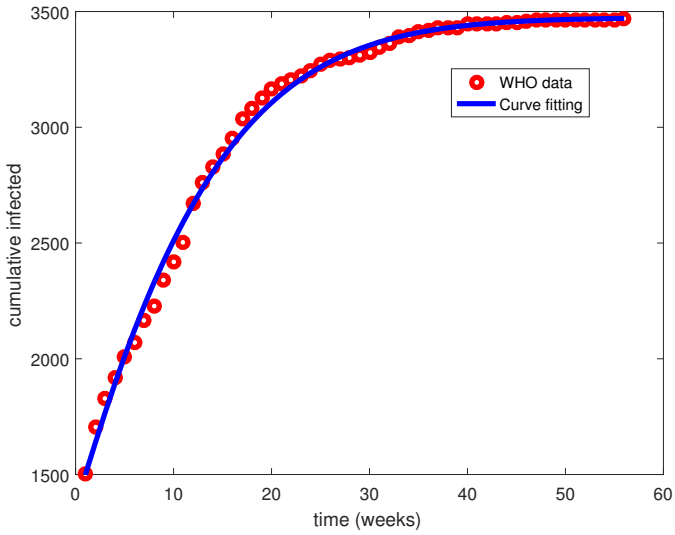

Fig. 3. Curve fitting to the real data reported during the 2018-2020 Kivu EVD outbreak. The parameters values are in Table 2 and the initial conditions are assumed $S(0) = 11,\ 000,\ 000$, $J(0) = 300, I(0) = 300, H(0) = 300, D(0) = 400, R(0) = 200, V(0) = 5$.

5.2. *Sensitivity of the parameter β_v*

The environment compartment has been neglected in several EVD models. Despite the fact that, the contribution of the environment to the control reproduction number is negligible, in this section, we deal on the potential impact of the transmission through the environment in the course of EVD outbreak. In Figure 4, we assumed that: (i) the value of β_v is equal to 4.07×10^{-8} (blue curve); (ii) the value of β_v is equal to 5.07×10^{-8} (cyan curve); (iii) the value of β_v is equal to 6.07×10^{-8} (magenta curve). Figure 4 shows that, a small variation of the parameter β_v have a great impact on the dynamics of EVD. Remarkably, when the value of β_v increases, the number of infected increases as well. This feature was also seen in.[9] Thus, the decontamination of the environment should be considered in order to control EVD. However, to the best of our knowledge, this measure has not yet be experimented against EVD.

5.3. *Efficiency of control strategies addressed in model* (2.3)

Let's recall that, our model has addressed three main control strategies against EVD: the isolation of infected cases, the safe burial of Ebola-deceased individuals and the vaccination. The impact of these strategies on EVD outbreaks is numerically investigated in this paragraph. Firstly, in Figures 5, 6 and 7, we observe that, the number of infected decreases as the control parameters σ_1, σ_2 and τ increase. In fact, increasing the parameters σ_1 and σ_2 will reduce the number of infected hos-

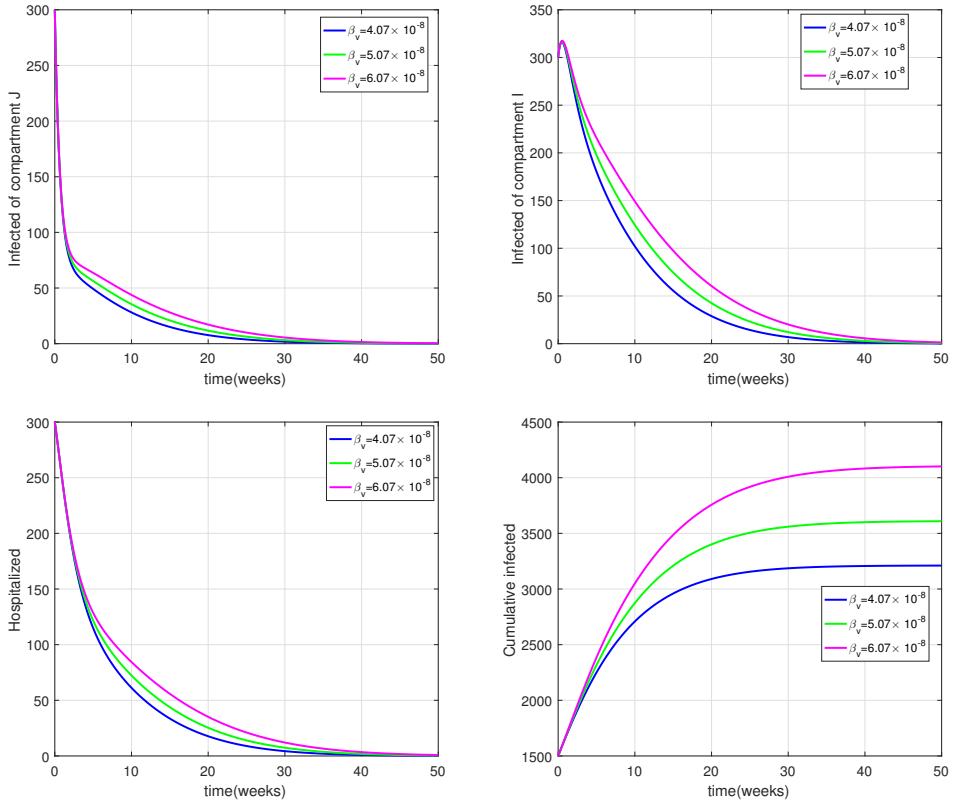

Fig. 4. Sensitivity of the parameter β_v: (i) $\beta_v = 0.04 \times 10^{-6}$ (blue curve); (ii) $\beta_v = 0.08 \times 10^{-6}$; (iii) (green curve) $\beta_v = 0.1 \times 10^{-6}$ (magenta curve). The other values for the simulations are in Table 2

pitalized, as well as the deceased who may continue to spread EVD, and increase the vaccination rate τ is an efficient measure which targets the susceptible population[9] and which can mitigate the level of the disease.[21] In particular, increasing the parameter σ_1 will reduce the impact of the modification parameter for the transmission during isolation (which have significant impact on the disease burden[24]). Note that, for $\sigma_1 = 0.03, \sigma_1 = 0.5$ and $\sigma_1 = 0.9$, one has $\mathcal{R}_c = 0.3475, \mathcal{R}_c = 0.33$ and $\mathcal{R}_c = 0.3217$, respectively. For $\sigma_2 = 0.03, \sigma_2 = 0.5$ and $\sigma_2 = 0.9$, one gets $\mathcal{R}_c = 0.4602, \mathcal{R}_c = 0.3765$ and $\mathcal{R}_c = 0.3052$, while for $\tau = 0.001, \tau = 0.01$ and $\tau = 0.05$, one obtains $\mathcal{R}_c = 0.4533, \mathcal{R}_c = 0.2573$ and $\mathcal{R}_c = 0.0927$ (the other parameters values are as in Table 2). This comforts the fact that, the safe burial and the vaccination have more impact than isolation at the beginning of the outbreak.

Moreover, the Figures 5, 6 and 7 suggest that, even in the course of EVD, safe burial and vaccination is more sensitive than the isolation. However, note that, for $\sigma_1 = 0.5$, the cumulative number of infected after 50 weeks is about 3, 450 (see Figure 5), while for $\sigma_2 = 0.5$ (see Figure 6) this number is about 4, 010. But, for

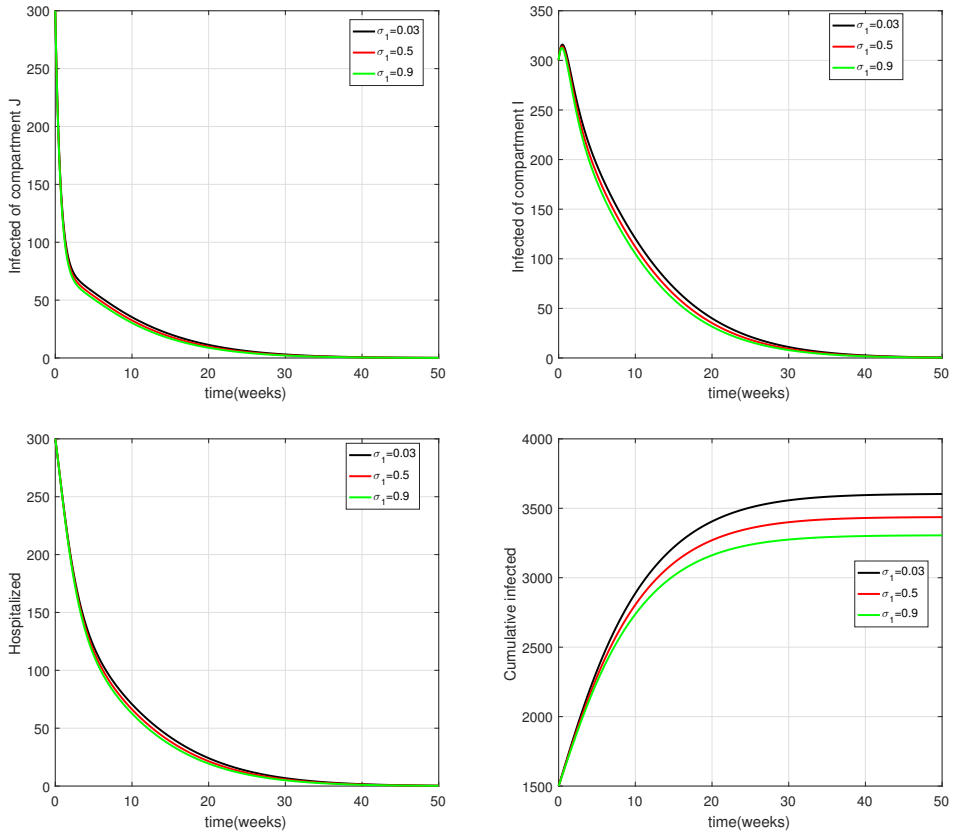

Fig. 5. Efficiency of the isolation: (i) $\sigma_1 = 0.03$ (black curve); (ii) $\sigma_1 = 0.5$ (red curve); (iii) $\sigma_1 = 0.9$ (green curve). The other values for the simulations are in Table 2.

$\sigma_1 = 0.9$, the cumulative number of infected after 50 weeks is 3, 300 and for $\sigma_2 = 0.9$ this number is 3, 100. In order to compare the usefulness of isolation, safe burial and vaccination in the course of EVD, we plot in Figures 8 and 9 the number of infected of the compartments J, I, H and the cumulative number of infected. In Figure 8, we consider: (i) $\sigma_1 = 0.5$ (magenta curve), (ii) $\sigma_2 = 0.5$ (red curve), (iii) $\tau = 0.05$ (blue curve). In Figure 9, we assume: (i) $\sigma_1 = 0.9$ (black curve), (ii) $\sigma_2 = 0.9$ (red curve), (iii) $\tau = 0.05$ (blue curve), keeping the other parameters constant. In the first figure, the isolation is better than the safe burial, but in the second we observe that the safe burial is more favourable than the isolation, in reducing the disease burden. Thus, the isolation and safe burial measures should not be neglected as far as EVD control is concerned. However, these two figures highlight that, the vaccination is more efficient than the two other control measures on the dynamics of EVD. This might justified the prominent place given to the vaccination during the 2018-2020 Kivu EVD outbreak.[19]

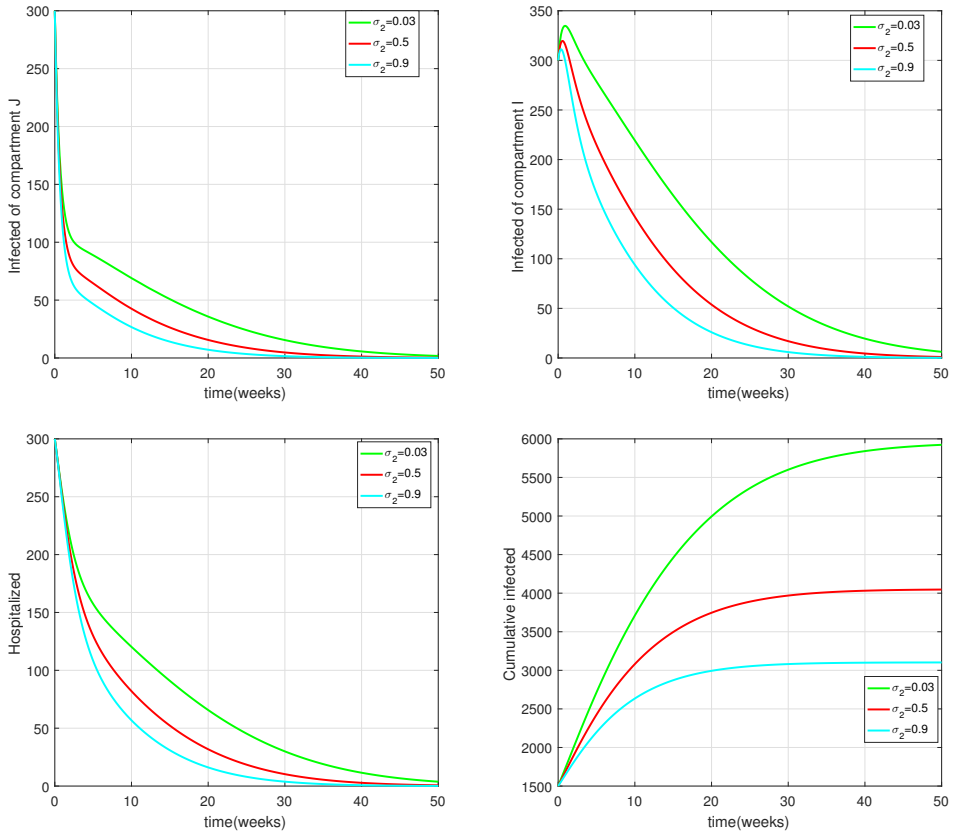

Fig. 6. Efficiency of the isolation: (i) $\sigma_2 = 0.1$ (green curve); (ii) $\sigma_2 = 0.4$ (red curve); (iii) $\sigma_2 = 0.7$ (cyan curve). The other values for the simulations are in Table 2

In the next paragraphs, we will explore the impact of other control measures, already implemented to mitigate EVD outbreaks.

5.4. *Impact of other control strategies*

Due to the high mortality rate of EVD, a plethora of control measures have been implemented by the health authorities. In this paragraph, we explore the importance of some of these strategies as supplement measures to those addressed in our model. Namely we assume that, the efforts are devoted to the implementation of the following supplement control strategies: (a) Strategy 1: the case finding; (b) Strategy 2: the educational campaigns; (c) Strategy 3: the combination of case finding and educational campaigns.

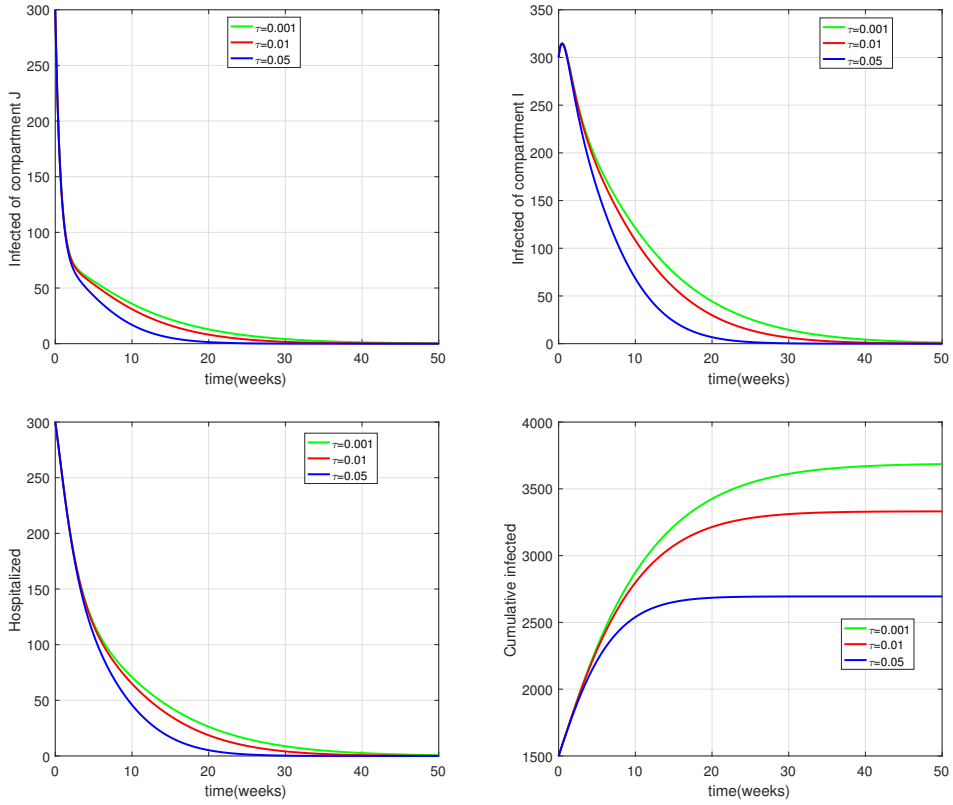

Fig. 7. Efficiency of the isolation: (i) $\tau = 0.001$ (green curve); (ii) $\tau = 0.005$ (red curve); (iii) $\tau = 0.01$ (blue curve). The other values for the simulations are in Table 2

5.4.1. ***Strategy 1: the case finding***

The case finding aims to find individuals showing EVD symptoms to bring them to isolation centers,[58,59] where they are separate from those who are healthy and undergo proper treatment.[34] Thus, an implementation of strategy 1, may increase the hospitalization rates η_j and η_i. This will have a favourable impact on the course of EVD outbreaks as we can see for instance in Figure 10, which is plotted when :(i) there is no case finding at all (blue curve), (ii) infected of compartment J and I are found and isolated at rate 0.2 per week (red curve), (iii) infected of compartment J and I are found at rate 0.4 per week (cyan curve). Namely, this figure shows that, as the case finding rate increases, the cumulative number of infected as well as those in compartments J and I decrease. But, the number of hospitalized increases during the first eight weeks. This may due to the fact that, the cases found are isolated (in compartment H). Figure 10 underscores the efficiency of this control strategy to mitigate the number of infected.

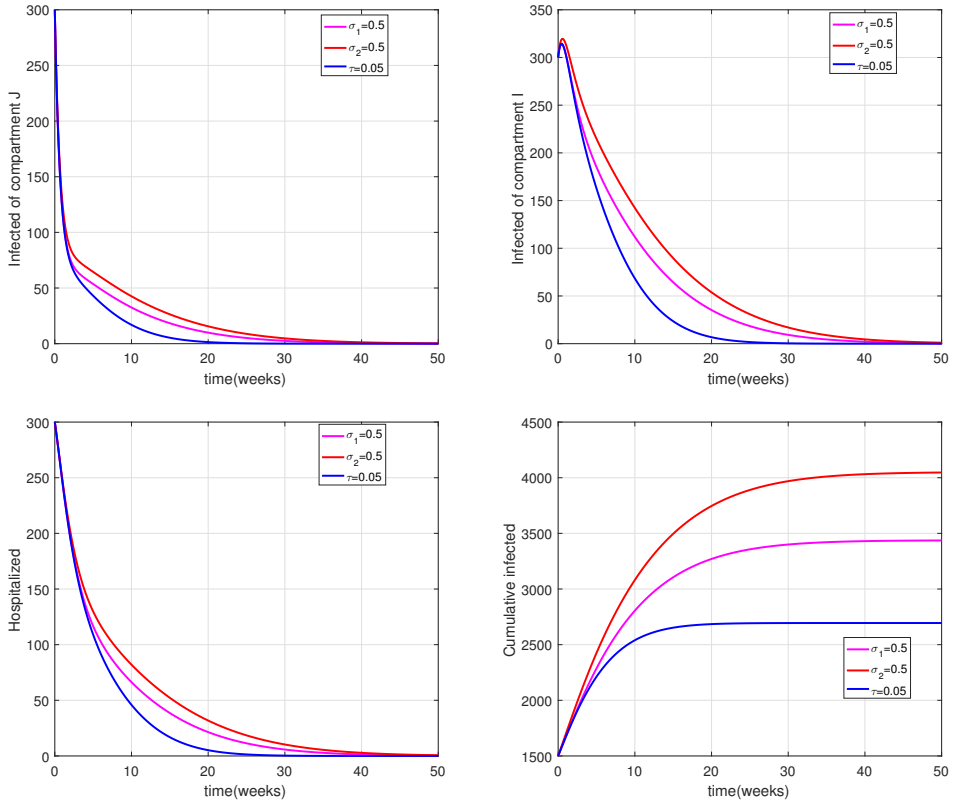

Fig. 8. Comparaison of the impact of isolation, safe burial and vaccination with the following parameters: (i) $\sigma_1 = 0.5$ (magenta curve); (ii) $\sigma_2 = 0.5$ (red curve); (iii) $\tau = 0.05$ (blue curve). The other values for the simulations are in Table 2

5.4.2. ***Strategy 2: educational campaigns***

During EVD outbreaks, educational campaigns are always implemented in order to increase the awareness of the population. Through this control measure, the population is well inform about EVD symptoms and develop cautiousness so that the reduction of contacts between susceptible and infectious individuals can occurs.[60,61] Through educational campaigns, the effective transmission rate of EVD for individuals in compartment J, I, H and D can be written as $\beta(1-e), \beta\nu_1(1-e), \beta\varepsilon(1-e)$ and $\beta\nu_2(1-e)$, where e measure the efficiency of this control strategy. In Figure 11, we assume for instance that: (i) $e = 0$ (black curve), (ii) $e = 0.2$ (cyan curve), (iii) $e = 0.4$ (magenta curve). This figure highlights that, the number of infected decreases as the impact of educational campaigns in the population increases and add credit to the usefulness of educational campaigns presented in.[60,61] In particular, the curve of the cumulative number of cases shows that after 50 weeks, the number of infected is respectively 3500 cases (for $e = 0$), 3125 cases (for $e = 0.2$)

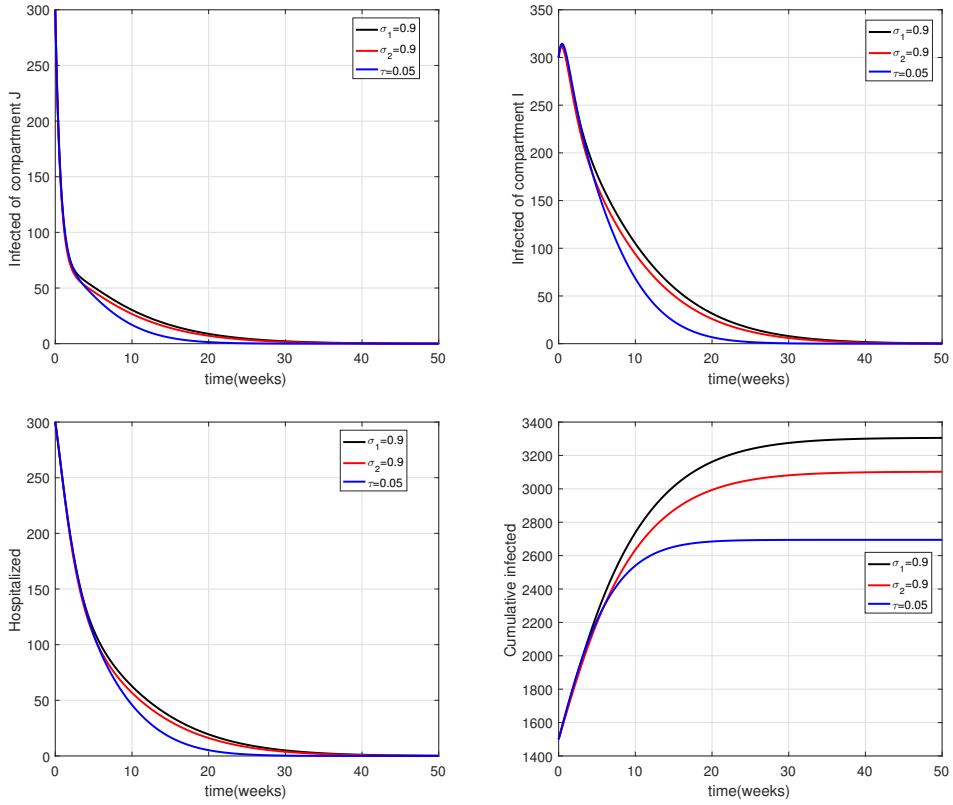

Fig. 9. Comparaison of the impact of isolation, safe burial and vaccination with the following parameters: (i) $\sigma_1 = 0.9$ (black curve); (ii) $\sigma_2 = 0.9$ (red curve); (iii) $\tau = 0.05$ (blue curve). The other values for the simulations are in Table 2

and 2900 cases (for $e = 0.4$), which are decreasing when the values of e increase.

5.4.3. *Combination of case finding and educational campaigns*

Due to the dangerousness of the Ebola virus, one should address the most effective control measure that can mitigate the dynamics of EVD. In this paragraph, we compare the efficiency of (i) case finding (at rate 0.4), (ii) educational campaigns ($e = 0.4$) and (iii) the combination of these two measures. Figure 12 suggests that, the case finding is more effective than the educational campaigns in reducing the level of the disease (see the cumulative curve), while a good combination of these two control measures is better than each of them taken separately, in the sense that the combination of these two measures will lead to a fewer number of cumulative cases. However note that, the combination of these two control measures seems to produce more hospitalized individuals than when the educational campaigns are implemented alone. This is due to the fact that, through this combination many

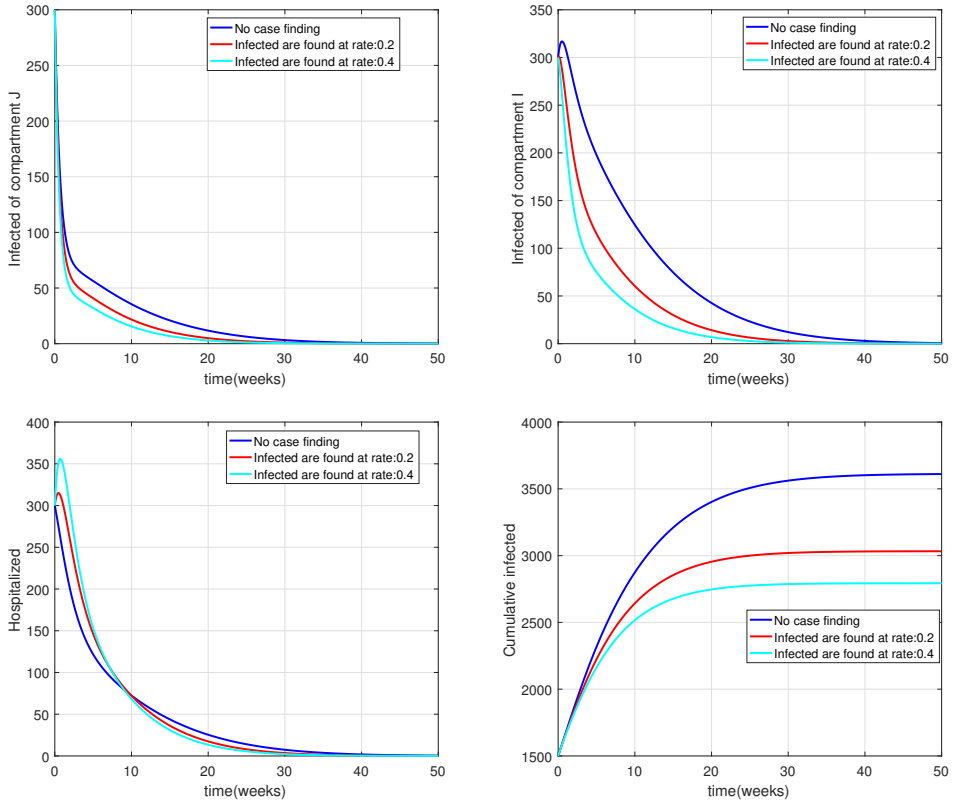

Fig. 10. Efficacy of the case finding measure. This figure is plotted when (i) there is no case finding (blue curve), (ii) infected of compartment J and I are found and isolated at rate 0.2 per week (red curve), (iii) infected of compartment J and I are found at rate 0.4 per week (cyan curve). The other values for the simulations are in Table 2

infected cases were tracked and isolated/hospitalized. This will consequently lead to an increase of their number.

6. Discussion and perspectives

In this paper, we have proposed a deterministic model to understand the spread of the Ebola virus disease. This model takes into account the transmission through a polluted environment and considers in addition the fact that, the immune system of individuals differs from each other and will lead either to severe or mild symptoms of the disease. However, those initially who begin to benign symptoms may progress to severe symptoms. A mathematical analysis of our model has been performed. Indeed, we have determined a threshold value $\mathcal{R}_c^c$ of the control reproduction number $\mathcal{R}_c$, below which the DFE is GAS, that is EVD dies out in the long run. Whenever the value of $\mathcal{R}_c$ ranges from $\mathcal{R}_c^c$ and 1, we have shown the existence

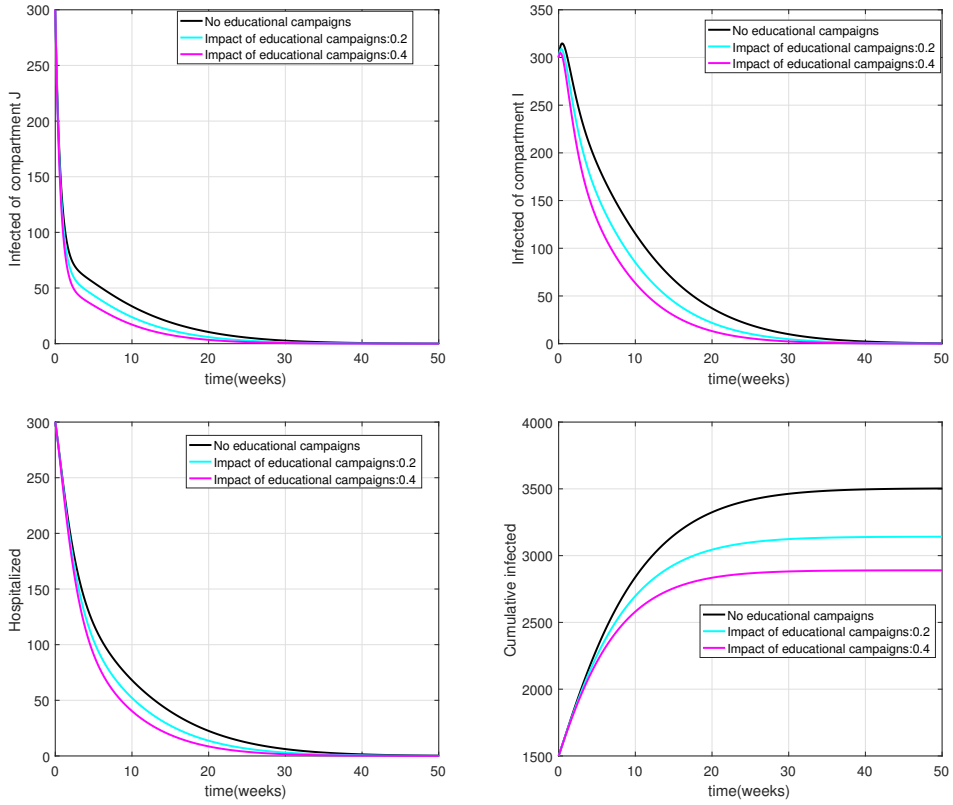

Fig. 11. Efficacy of educational campaigns. This is plotted when (i) there is no educational campaigns, (ii) (black curve) the impact of educational campaigns is equal to 0.2 (cyan curve), (iii) the impact of educational campaigns is equal to 0.4 per week (magenta curve). The other values for the simulations are in Table 2

of a backward bifurcation phenomenon, which corresponds to the case where a LAS positive equilibrium co-exists with the DFE, which is also LAS. The existence of this bifurcation makes the control of EVD difficult, since the requirement of $\mathcal{R}_c$ below one, although necessary is not sufficient for the elimination of EVD, more efforts need to be deploy. When the value of $\mathcal{R}_c$ is greater than one, we prove the existence of a unique endemic equilibrium, LAS. That is the disease may persist and can be endemic. We have validated our model by fitting it to the available data for the 2018-2020 Kivu EVD outbreak. From our parameters estimated, the value of the control reproduction number is 0.33 for this outbreak. This relatively low value of the control reproduction number may be due to the great experience DRC has in the fighting against EVD, knowing that the country had faced many outbreaks and has developed efficient means to protect its population. For instance, without the account of vaccination in our model (that is for $\tau = 0$), the control reproduction number of our model were be equal to 0.48, which is near to 0.51, obtained after

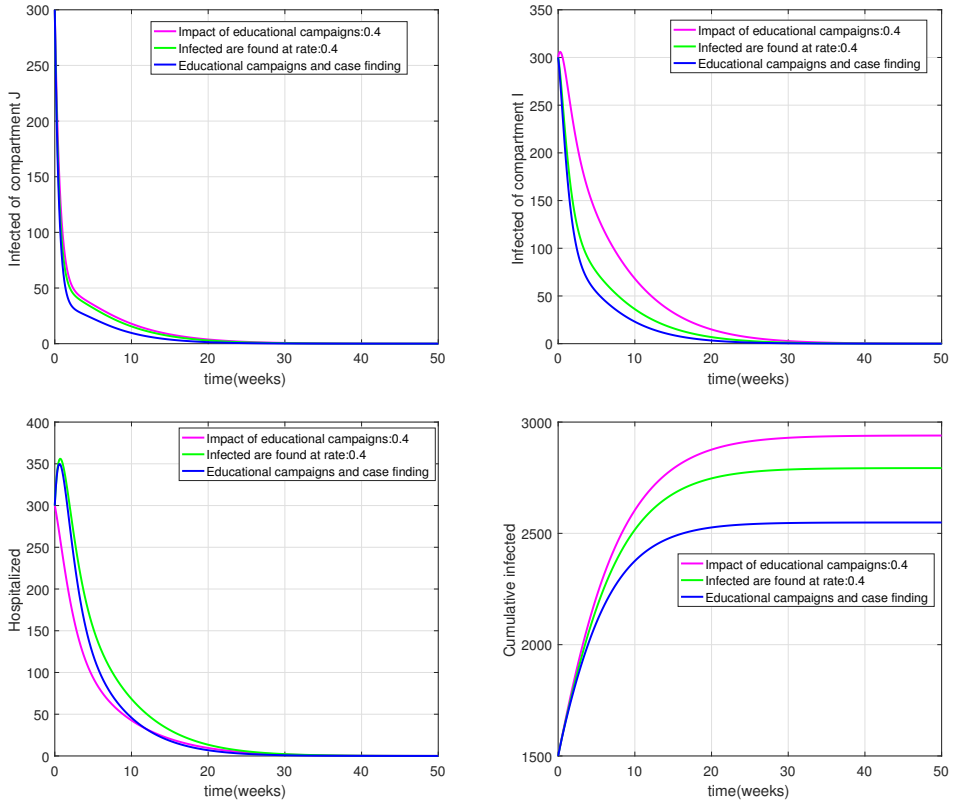

Fig. 12. Combination of case finding and educational campaigns. This figure is plotted when: (i) the case finding only is (ii) implemented at rate: 0.4 (cyan curve), the impact of educational campaigns is equal to 0.4 (magenta curve) and there is (iii) no case finding the two former measures are addressed (blue curve). The other values for the simulations are in Table 2

intervention in DRC in 1995 (during which vaccine were not available).[57]

Moreover, our estimated values have shown that, one should reduce the transmission through contacts with individuals showing severe symptoms in order to control EVD quickly. Furthermore, we have proven that, the dynamics of EVD is sensitive to the effective transmission through a polluted environment. This comforts the fact that, this transmission route may increase the level of EVD.[9] Besides, we have quantitatively investigated the usefulness of isolation, safe burial and vaccination in the course of EVD outbreak. In this regard, our main observation is that, the vaccination measures is more efficient than the isolation and the safe burial. This might justified the prominent place given to the vaccination during the 2018-2020 Kivu EVD outbreak.[19] Besides, in order to mitigate, the impact of the transmission of EVD due to contact with infected who are outside hospital, we have explored numerically the usefulness of the case finding[58,59] (which has been already addressed to fight against EVD) and educational campaigns[61] as a supplement measures to

isolation, safe burial (which concerns the deceased formerly infected by EVD) and vaccination. Our results have shown that, the case finding is better than the educational campaigns to reduce the level of EVD, but a good combination of these control measures is better than each of them taken separately.

Despite the relevance of our study, let us recognize that, our model did not take into account the spillover event from animals to humans, since this fact is already underscore in our previous works.[9,47] Moreover, the delay in the management of infected has been underestimated, this aspect can be useful since the early diagnosis of EVD infected improves the survival rate.[13] Furthermore, in spite of the account of the vaccination in our model, we have not explored the number of cases and deaths that may be avoided by this measure. The authors in[62] think for instance that, when 10% of health care workers get vaccination, 54% of cases and 51% of deaths can be avoided. Finally let's recall that, misconceptions[63] and ignorance about EVD in Africa remain a serious matter and should be explored in order to control EVD. These drawbacks will be our focus in a nearest future. In particular, we intend firstly to develop an EVD model which considers the impact of misconceptions[63] and educational campaigns to control EVD outbreaks.[60] In fact in the model presented in this paper, the modern medicine appears as the only means of treatment. Considering the African context, this is not always the case, because many people link EVD to witchcraft or the punishment of God for the corruption of the humanity.[10] Secondly, we will propose an Ebola model which will focus on the effects of timing of interventions.[6] Indeed the 2013-2015 EVD outbreak has started in December 2013, but it is only in March 2014 that it has been diagnosed. This diagnostic delay has substantially impacted the spread of the disease and need to be considered shortly. Thirdly, we shall formulate and analyse a model which considers differential susceptibility in the population,[21] the presence of super spreaders of EVD (the healthcare workers)[62] and ring vaccination. Finally, we will propose a model which takes into account an hypothetical co-infection: Ebola-COVID-19 (Ebola occurred in DRC and Guinea in February 2021, where the COVID-19 prevailed[2]). Namely, we will investigate the impact of COVID-19 on the rapid control of EVD. This is motivated by the fact that the last EVD outbreaks were rapidly eliminated, perhaps the measures taken to limit the spread of COVID-19 may have served to curtail and to eliminate EVD.

Conflict of interest

The authors declare that they have no conflict of interest.

Appendices

Appendix A: Proof the the well-posedness of the model

Proof of Theorem 3.1

We begin by proving that, if $S(0) > 0$ then $\forall\, t > 0, S(t) > 0$. Suppose $S(0) > 0$. The integration from 0 to t of the first equation of (2.4) yields:

$$S(t) = \left[S(0) + \int_0^t \pi exp\left(\int_0^s (\lambda(u) + \mu)du\right) ds\right] \times exp\left(\int_0^t -(\lambda(u) + \mu)du\right).$$

Thus, $S(t) > 0\ \forall\, t > 0$.

Assume besides that, $J(0) \geq 0, I(0) \geq 0, H(0) \geq 0, D(0) \geq 0, R(0) \geq 0$ and $V(0) \geq 0$. If for instance J becomes zero at a time t before I, H, D, R and V become zero, then from the second equation of (2.4), $\dot{J}(t) = \lambda(t)S(t) \geq 0$ at t_1. Thus, $J(t)$ is a non-decreasing function of t at t_1. Therefore, $J(t)$ stays non-negative. Similarly, it can be shown that, I, H, D, R and V stay non-negative for non-negative initial conditions.

Proof of Theorem 3.2

Straightforward computations show that,

$$\dot{M}(t) = \pi - \mu(S + R) - \delta_j J - \delta_i I - \delta_h H. \tag{6.1}$$

Since $\mu \leq \min\{\delta_j, \delta_i, \delta_h\}$, one has

$$\dot{M}(t) \leq \pi - \mu M \tag{6.2}$$

Thus, following Gronwall lemma,

$$M(t) \leq \frac{\pi}{\mu} + \left(M(0) - \frac{\pi}{\mu}\right) e^{-\mu t}. \tag{6.3}$$

Besides, from (6.1), one gets

$$\dot{M}(t) \geq \pi - (\mu + \delta_j + \delta_i + \delta_h)M \tag{6.4}$$

Thus,

$$M(t) \geq \frac{\pi}{(\mu + \delta_j + \delta_i + \delta_h)} + \left(M(0) - \frac{\pi}{(\mu + \delta_j + \delta_i + \delta_h)}\right) e^{-(\mu+\delta_j+\delta_i+\delta_h)t}. \tag{6.5}$$

If $M(0) > \dfrac{\pi}{\mu}$, then $\dot{M}(t) < 0$. So, from the inequality (6.3), $M(t)$ decreases until reaching $\dfrac{\pi}{\mu}$ when t tends to ∞. Similarly, if $M(0) < \dfrac{\pi}{(\mu + \delta_j + \delta_i + \delta_h)}$, then from the inequality (6.4), $M(t)$ increases until reaching a maximum $\dfrac{\pi}{(\mu + \delta_j + \delta_i + \delta_h)}$, when t tends to ∞.

Moreover, if

$$\frac{\pi}{(\mu + \delta_j + \delta_i + \delta_h)} \leq M(0) \leq \frac{\pi}{\mu},$$

then since one has

$$\frac{\pi}{(\mu+\delta_j+\delta_i+\delta_h)}+\left(M(0)-\frac{\pi}{(\mu+\delta_j+\delta_i+\delta_h)}\right)e^{-(\mu+\delta_j+\delta_i+\delta_h)t}\leq M(t)\leq\frac{\pi}{\mu}+\left(M(0)-\frac{\pi}{\mu}\right)e^{-\mu t},$$

one concludes that

$$\frac{\pi}{(\mu+\delta_j+\delta_i+\delta_h)}\leq M(t)\leq\frac{\pi}{\mu},\ \forall\, t>0.$$

Similarly, it can be shown that,

$$\frac{\pi(\delta_j+\delta_i+\delta_h)}{b(\mu+\delta_j+\delta_i+\delta_h)}\leq D(t)\leq\frac{\pi(\delta_j+\delta_i+\delta_h)}{b\mu},\ \forall\, t\geq 0,$$

and $\forall\, t\geq 0$,

$$\frac{b\pi(q_1+q_2+q_3)+q_4\pi(\delta_j+\delta_i+\delta_h)}{ub(\mu+\delta_j+\delta_i+\delta_h)}\leq V(t)\leq\frac{b\pi(q_1+q_2+q_3)+q_4\pi(\delta_j+\delta_i+\delta_h)}{ub\mu}.$$

Thus, the set Ω is positively invariant and absorbing.

Appendix B: Determination of the equilibria of the Model (2.3)

Let $E^*=(S^*,J^*,I^*,H^*,D^*,R^*,V^*)$ an equilibrium of System (2.4). Its components S^*, J^*, I^*, H^*, D^*, R^* and V^* are the solutions of the following system of equations:

$$\begin{cases}\pi-\lambda^*S-\theta_2S^*=0,\\ p\lambda^*S^*-\phi_1J^*=0,\\ (1-p)\lambda^*S^*+\alpha J^*-\phi_2I^*=0,\\ \eta_jJ^*+\eta_iI^*-\phi_3H^*=0,\\ \delta_jJ^*+\delta_iI^*+\delta_hH^*-bD^*=0,\\ \theta_1S^*+\gamma_jJ^*+\delta_iI^*+\gamma_hH^*-\mu R^*\\ q_1J^*+q_2I^*+q_3H^*+q_4D-uV^*=0.\end{cases}\tag{6.6}$$

where

$$\lambda^*=\frac{\beta(J^*+\sigma_hH^*+\nu_1I^*+\sigma_dD^*)}{N^*}+\beta_vV^*,\tag{6.7}$$

and

$$N^*=S^*+J^*+I^*+H^*+D^*+R^*.\tag{6.8}$$

Simple computations show that,

$$S^*=\frac{\pi}{\lambda^*+\theta_2},\qquad J^*=\frac{p\pi\lambda^*}{\phi_1(\lambda^*+\theta_2)},\qquad I^*=\frac{\pi\lambda^*k_2}{\phi_1\phi_2(\lambda^*+\theta_2)},$$

$$H^*=\frac{\pi\lambda^*k_3}{\phi_1\phi_2\phi_3(\lambda^*+\theta_2)},\ D^*=\frac{\pi\lambda^*k_4}{b\phi_1\phi_2\phi_3(\lambda^*+\theta_2)},\ R^*=\frac{\theta_1\pi\phi_1\phi_2\phi_3+\pi\lambda^*k_5}{\mu\phi_1\phi_2\phi_3(\lambda^*+\theta_2)}.$$

Substituting these expressions into (6.8) lead to:

$$N^*=\frac{\pi b\mu\phi_1\phi_2\phi_3+b\theta_1\pi\phi_1\phi_2\phi_3+\pi\lambda^*k_6}{\mu b\phi_1\phi_2\phi_3(\lambda^*+\theta_2)}.$$

Putting these relationships into the expression of λ^* gives

$$\lambda^* = 0 \text{ or } (E) : A_2\lambda^{*2} + A_1\lambda^* + A_0 = 0.$$

where

$$\begin{aligned}
A_2 &= u\pi bk_6\phi_1\phi_2\phi_3,\\
A_1 &= u\pi b^2\phi_1^2\phi_2^2\phi_3^2\theta_2 + \pi k_6\theta_2 ub\phi_1\phi_2\phi_3 - \beta_v\pi^2k_7k_6\\
&\quad -\beta\pi\mu ub\phi_1\phi_2\phi_3(pb\phi_2\phi_3 + \nu_1k_2\phi_3b + \sigma_hk_3b + \sigma_dk_4)\\
A_0 &= \theta_2^2ub^2\phi_1^2\phi_2^2\phi_3^2\pi - \theta_2\beta\pi\mu ub\phi_1\phi_2\phi_3(p\phi_2\phi_3b + \nu_1k_2\phi_3b + \sigma_hk_3b + \sigma_dk_4)\\
&\quad -\phi_1\phi_2\phi_3\pi^2b\beta_vk_7\theta_2.
\end{aligned}$$

$\lambda^* = 0$ leads to the disease-free equilibrium (DFE) $E_0 = (S_0, 0, 0, 0, 0, R_0, 0)$ with $S_0 = \dfrac{\pi}{\theta_2}$, $R_0 = \dfrac{\pi\theta_1}{\mu\theta_2}$.

Assume in the sequel that $\lambda^* \neq 0$. Note that, A_0 can be written such as

$$A_0 = \pi b^2\theta_2^2u\phi_1^2\phi_2^2\phi_3^2(1 - \mathcal{R}_c),$$

where

$$\mathcal{R}_c = \frac{\beta\mu(p\phi_2\phi_3b + \nu_1k_2\phi_3b + \sigma_hk_3b + \sigma_dk_4)}{b\theta_2\phi_1\phi_2\phi_3} + \frac{\beta_vk_7\pi}{bu\theta_2\phi_1\phi_2\phi_3}.$$

It is clear that, when $\mathcal{R}_c > 1$ the Model (2.3) has a unique endemic equilibrium.

Assume $\mathcal{R}_c < 1$. The discriminant Δ of the equation (E) gives:

$$\Delta(\mathcal{R}_c) = A_1^2 - 4A_2\pi b^2u\theta_2^2\phi_1^2\phi_2^2\phi_3^2(1 - \mathcal{R}_c)$$

Thus,

$$\Delta(\mathcal{R}_c) = 0 \Leftrightarrow \mathcal{R}_c^c = 1 - \frac{A_1^2}{4A_2\pi b^2u\theta_2^2\phi_1^2\phi_2^2\phi_3^2}.$$

Therefore, our model has two positive equilibria if $\mathcal{R}_c^c < \mathcal{R}_c < 1$ and a unique positive equilibrium for $\mathcal{R}_c < \mathcal{R}_c^c$.

Appendix C: Proof of the global asymptotic stability of the disease-free equilibrium

We rewrite the Model (2.3) as

$$\begin{cases} \dfrac{dX}{dt} = F(X, Y) \\ \dfrac{dY}{dt} = G(X, Y),\ G(X, 0) = 0 \end{cases} \tag{6.9}$$

where $X = (S, R) \in \mathbb{R}^2$ and $Y = (J, I, H, D, V) \in \mathbb{R}^5$, with the components of $X \in \mathbb{R}^2$ denoting the non-infected population, and the components $Y \in \mathbb{R}^5$ denoting the infected population.

The DFE E_0 is denoted here as $E_0 = (X^*, 0)$, $X^* = (S_0, R_0)$.

The DFE is globally asymptotically stable if the following two conditions are satisfied:[48,64]

1. For the system $\dfrac{dX}{dt} = F(X, 0)$, X^* is GAS.
2. $G(X, Y) = BY - \hat{G}(X, Y)\ \hat{G}(X, Y) \geq 0$ for $(X, Y) \in \Omega$, where $B = D_Y G(X^*, 0)$ is a Metzler matrix and Ω is defined in Proposition 3.2

From the System (2.3), one can easily see that,

$$B = \begin{pmatrix} p\beta - \phi_1 & p\beta\nu_1 & p\beta\sigma_h & p\beta\sigma_d & p\beta_v\dfrac{\pi}{\mu} \\ (1-p)\beta + \alpha & (1-p)\beta\nu_1 - \phi_2 & (1-p)\beta\sigma_h & (1-p)\beta\sigma_d & (1-p)\beta_v\dfrac{\pi}{\mu} \\ \eta_j & \eta_i & -\phi_3 & 0 & 0 \\ \delta_j & \delta_i & \delta_h & -b & 0 \\ q_1 & q_2 & q_3 & q_4 & -u \end{pmatrix},$$

$$\hat{G}(X, Y) = \begin{pmatrix} p\left[\beta J\left(1 - \dfrac{S}{N}\right) + \beta\nu_1 I\left(1 - \dfrac{S}{N}\right) + \beta\sigma_h H\left(1 - \dfrac{S}{N}\right) + \beta\sigma_d D\left(1 - \dfrac{S}{N}\right) + \beta_v V\left(\dfrac{\pi}{\mu} - S\right)\right] \\ (1-p)\left[\beta J\left(1 - \dfrac{S}{N}\right) + \beta\nu_1 I\left(1 - \dfrac{S}{N}\right) + \beta\sigma_h H\left(1 - \dfrac{S}{N}\right) + \beta\sigma_d D\left(1 - \dfrac{S}{N}\right) + \beta_v V\left(\dfrac{\pi}{\mu} - S\right)\right] \\ 0 \\ 0 \end{pmatrix}.$$

Clearly, $\hat{G}(X, Y) \geq 0$ for $(X, Y) \in \Omega$. Moreover, it is evident that, X^* is GAS for the system $\dfrac{dX}{dt} = F(X, 0)$. Therefore, following the Theorem of Castillo-Chavez et al. presented in[48,64] the DFE of Model (2.3) is GAS when $\mathcal{R}_c < \mathcal{R}_c^c$.

Appendix D: Proof of the local asymptotic stability of the Endemic equilibrium

To prove the Theorem 3.3, we use the Center Manifold Theory.

Let's β as the bifurcation parameter. It is clear that, there exists $\sigma_v \in \mathbb{R}^+$ such that, $\beta_v = \beta\sigma_v$. Thus, the critical value of β at $\mathcal{R}_c = 1$ is given by:

$$\beta^* = \frac{\theta_2 u\phi_1\phi_2\phi_3}{\mu u(p\phi_2\phi_3 b + \nu_1 k_2\phi_3 b + \sigma_h k_3 b + \sigma_d k_4) + \sigma_v k_7\pi}.$$

To investigate the stability of the unique endemic equilibrium, let's make the following change of model variables

$$x_1 = S, \quad x_2 = J, \quad x_3 = I, \quad x_4 = H, \quad x_5 = D, \quad x_6 = R, \quad x_7 = V.$$

Then the System (2.3) can be rewritten in the form

$$\frac{dy}{dt} = f(y),$$

with $f = (f_1, f_2, f_3, f_4, f_5, f_6, f_7)$, such as:

$$\begin{cases} f_1 = \pi - \beta \left(\dfrac{x_2 + \sigma_h x_4 + \nu_1 x_3 + \sigma_d x_5}{x_1 + x_2 + x_3 + x_4 + x_6} + \sigma_v x_7 \right) x_1 - \theta_2 x_1, \\ f_2 = p\beta \left(\dfrac{x_2 + \sigma_h x_4 + \nu_1 x_3 + \sigma_d x_5}{x_1 + x_2 + x_3 + x_4 + x_6} + \sigma_v x_7 \right) x_1 - \phi_1 x_2, \\ f_3 = (1-p)\beta \left(\dfrac{x_2 + \sigma_h x_4 + \nu_1 x_3 + \sigma_d x_5}{x_1 + x_2 + x_3 + x_4 + x_6} + \sigma_v x_7 \right) x_1 + \alpha\, x_2 - \phi_2 x_3, \\ f_4 = \eta_j x_2 + \eta_i x_3 - \phi_3 x_4, \\ f_5 = \delta_j x_2 + \delta_i x_3 + \delta_h x_4 - b x_5, \\ f_6 = \theta_1 x_1 + \gamma_j x_2 + \gamma_i x_3 + \gamma_h x_4 - \mu\, x_6, \\ f_7 = q_1 x_2 + q_2 x_3 + q_3 x_4 + q_4 x_5 - u x_7, \end{cases} \tag{6.15}$$

The Jacobian matrix J_* for the System (6.15) at the DFE E_0 when $\beta = \beta^*$ is given by:

$$J_* = \begin{pmatrix} -\theta_2 & -\frac{\beta^* S_0}{N_0} & -\frac{\beta^* \nu_1 S_0}{N_0} & -\frac{\beta^* \sigma_h S_0}{N_0} & -\frac{\beta^* \sigma_d S_0}{N_0} & 0 & -\beta^* \sigma_v S_0 \\ 0 & \frac{p\beta^* S_0}{N_0} - \phi_1 & \frac{p\beta^* \nu_1 S_0}{N_0} & \frac{p\beta^* \sigma_h S_0}{N_0} & \frac{p\beta^* \sigma_d S_0}{N_0} & 0 & p\beta^* \sigma_v S_0 \\ 0 & \frac{(1-p)\beta^* S_0}{N_0} + \alpha & \frac{(1-p)\beta^* \nu_1 S_0}{N_0} - \phi_2 & \frac{(1-p)\beta^* \sigma_h S_0}{N_0} & \frac{(1-p)\beta^* \sigma_d S_0}{N_0} & 0 & (1-p)\beta^* \sigma_v S_0 \\ 0 & \eta_j & \eta_i & -\phi_3 & 0 & 0 & 0 \\ 0 & \delta_j & \delta_i & \delta_h & -b & 0 & 0 \\ \theta_1 & \gamma_j & \gamma_i & \gamma_h & 0 & -\mu & 0 \\ 0 & q_1 & q_2 & q_3 & q_4 & 0 & -u \end{pmatrix}$$

One can easily seen that the Jacobian J_* of System (6.15) at the DFE E_0, with $\beta = \beta^*$, has zero as a simple eigenvalue (with all other eigenvalues having negative real parts). Hence, the Center Manifold theory method[65] can be used to determine the local stability of the endemic equilibrium of System (6.15) near the bifurcation parameter $\beta = \beta^*$.

One can show that the components of a right-eigenvector $w = (w_1, w_2, w_3, w_4, w_5, w_6, w_7)^T$ and a left-eigenvector $m = (m_1, m_2, m_3, m_4, m_5, m_6, m_7)^T$ of J_* associated to the zero eigenvalue are given by the following two systems:

$$\begin{cases} w_1 = -\dfrac{\beta^* S_0}{N_0 \theta_2}(w_2 + \nu_1 w_3 + \sigma_h w_4 + N_0 \sigma_v w_7), \quad w_2, w_3, w_6 > 0 \\ w_4 = \dfrac{1}{\phi_3}(\eta_j w_2 + \eta_i w_3), \quad w_5 = \dfrac{1}{b\phi_3}[(\delta_h \eta_j + \phi_3 \delta_j) w_2 + (\delta_h \eta_i + \phi_3 \delta_i) w_3], \\ w_7 = \dfrac{1}{b\phi_3 u}[w_2(\delta_h \eta_j + \phi_3 \delta_j + b\phi_3 q_1 + b q_3 \eta_j) + w_3(\delta_h \eta_i + \phi_3 \delta_i + b\phi_3 q_2 + b q_3 \eta_i)] \end{cases}$$

and

$$\begin{cases} m_1 = 0, \quad m_6 = 0, \quad m_2, m_3 > 0, \\ m_4 = \dfrac{\beta S_0 (p m_2 + (1-p) m_3)}{N_0 \phi_3 u b}[\sigma_h u b + \delta_h(\sigma_d u + \sigma_v q_4 N_0) + \sigma_v q_3 N_0 b], \\ m_5 = \dfrac{\beta S_0 (p m_2 + (1-p) m_3)}{N_0 u b}(\sigma_d u + \sigma_v q_4 N_0), \quad m_7 = \dfrac{\beta \sigma_v S_0}{u}(p m_2 + (1-p) m_3). \end{cases}$$

$$a = \sum_{k,i,j=1}^{7} m_k w_i w_j \frac{\partial^2 f_k}{\partial x_i \partial x_j}(0,0), \quad \text{and} \quad d = \sum_{k,i=1}^{7} m_k w_i \frac{\partial^2 f_k}{\partial x_i \partial \beta^*}(0,0),$$

are given by:

$$\begin{aligned} a = {} & 2\beta^* w_1 m_2 p(R_0 N_0^{-2} w_2 + \nu_1 R_0 N_0^{-2} w_3 + \sigma_h R_0 N_0^{-2} w_4 + \sigma_d R_0 N_0^{-2} w_5 + \sigma_v w_7) \\ & -2m_2 \beta^* N_0^{-2} S_0 p[(1+\nu_1) w_2 w_3 + (1+\sigma_h) w_2 w_4 + (1+\sigma_d) w_2 w_5 + w_2^2 + \nu_1 w_3^2 \\ & +\sigma_h w_4^2 + \sigma_d w_5^2 + w_6(w_2 + \nu_1 w_3 + \sigma_h w_4 + \sigma_d w_5) + (\nu_1 + \sigma_h) w_3 w_4 \\ & +(\nu_1 + \sigma_d) w_3 w_5 + (\sigma_h + \sigma_d) w_4 w_5] + 2\beta^* w_1 m_3 (1-p)(R_0 N_0^{-2} w_2 + \nu_1 R_0 N_0^{-2} w_3 \\ & +\sigma_h R_0 N_0^{-2} w_4 + \sigma_d R_0 N_0^{-2} w_5 + \sigma_v w_7) - 2m_3 \beta^* N_0^{-2} S_0 (1-p)[(1+\nu_1) w_2 w_3 \\ & +(1+\sigma_h) w_2 w_4 + (1+\sigma_d) w_2 w_5 + w_2^2 + \nu_1 w_3^2 + \sigma_h w_4^2 + \sigma_d w_5^2 + w_6(w_2 + \nu_1 w_3 \\ & +\sigma_h w_4 + \sigma_d w_5) + (\nu_1 + \sigma_h) w_3 w_4 + (\nu_1 + \sigma_d) w_3 w_5 + (\sigma_h + \sigma_d) w_4 w_5] \\ < {} & 0, \text{ since } w_1 < 0, \end{aligned}$$

and

$$d = S_0 \, N_0^{-1} \, [pm_2 + (1-p)m_3] \, (w_2 + \nu_1 w_3 + \sigma_h w_4 + \sigma_d w_5 + \sigma_v N_0 w_7) > 0.$$

Then, the unique endemic equilibrium of Model (2.4) is locally asymptotically stable when $\mathcal{R}_c > 1$, but near to 1. Moreover, the bifurcation of the System (2.4) around $\mathcal{R}_c = 1$ is trans-critical.

Acknowledgement

The authors would like to thank the two reviewers and the handling editor for their constructive comments and suggestions which substantially improved the quality of this manuscript.

References

1. Ebola Outbreak - Democratic Republic of the Congo, 2019. https://wwww.who.int/emergencies/situations/Ebola-2019-drc.
2. MSF, DRC's Twelft Ebola Outbreak, 2021. http://www.msf.org/drc-ebola-outbreak-crisis-update.
3. F. B. Agusto, Mathematical model of Ebola transmission dynamics with relapse and reinfection, *Math. Biosci.* 283:48–59, 2017.
4. D. Salem, R. Smith, A Mathematical Model of Ebola Virus Disease: Using Sensitivity Analysis to Determine Effective Intervention Targets, *SCSC'16: Proceedings of the Summer Computer Simulation Conference* 1–8, 2016.
5. S. J. Chapman, V. S. Hill, Human Genetic Susceptibility to Infectious Disease, *Nature Reviews Genetics* 13(3):175–188, 2012.
6. J. Ponce, Y. Zheng, G. Lin, Z. Feng, Assessing the Effects of Modeling the Spectrum of Clinical Symptoms on the Dynamics and Control of Ebola, *J. Theor. Biol* 467:111–122, 2019.
7. A. L. Rasmussen, A. Okumara, M. T. Ferris, R. Green, F. Feldmann, S. M. Kelly, D. P. Scott, D. Safronetz, E. Haddock, R. LaCasse, M. J. Thomas, P. Sova, V. S. Carter, J. M. Weiss, D. R. Miller, G. D. Shaw, M. J. Korth, M. T. Heise, R. S. Baric, F. Villena, M. G. Katze, Host Genetic Diversity Enables Ebola Haemorrhagic Fever Pathogenesis and Resistance, *Science* 346(6212):987–991, 2014.

8. A. Sanchez, K. E. Wagoner, P. E. Rollin, Sequence-Based Human Leukocyte Antigen-B Typing of Patients Infected with Ebola Virus in Uganda in 2000: Identification of Alleles Associated with Fatal and non Fatal Disease Outcomes, *J. Infect. Dis.* 196:S329–336, 2007.
9. T. Berge, J. S. -M. Lubuma, A. J. O. Tassé, H. M. Tenkam, Dynamics of Host-Reservoir Transmission of Ebola with Spillover Potential to Humans, *Electron J Qual Theory Differ. Equ.* 14:1–32, 2018.
10. S. D. D. Njankou, Mathematical Models of Ebola Virus Disease with Socio-Economics Dynamics, Ph.D thesis, *University of Stellenbosch, South Africa*, 2019.
11. Y. Li, H. Wang, Y-G. Wang, Experiences and Challenges in the Health Protection of Medical Teams in the Chinese Ebola Treatment Center, Liberia: a Qualitative Study, *Infect. Dis. Poverty* 7:92:1–12, 2018.
12. WHO, Ebola Virus Disease, 2019. https://www.who.int/newsroom/fact-sheets/-detail/ebola-virus-disease.
13. Ebola (Ebola Virus Disease) Treatment, *CDC*, 2021. https://cdc.gov/vhf/ebola/treatment/index.html.
14. I. Area, F. Ndaïrou, J. J. Nieto, C. J. Silva, D. F. M. Torres, Ebola Model and Optimal Control with Vaccination Constraints, *J. Ind. Manag. Optim* 278:1–21, 2017.
15. S. Merler, M. Ajelli, L. Fumanelli, S. Parlamento, A. P. Y. Piontti, N. E. Dean, G. Putoto, D. Carraro, I. M. Longini, J. M. E. Halloran, A. Vespignani, Containing Ebola at the Source with Ring Vaccination, *PLOS Negl. Trop. Dis* 10(11):1–11, 2016.
16. D. Branigan, Evidence shows Ring Vaccination Strategy Effective in Limiting Ebola Outbreak in DRC, *Health Policy Watch*, 15-04-2019. https://www.healthpolicy-watch.org/evidence-shows-ring-vaccination-strategy-effective-in-limiting-ebola-outbreak-in-drc.
17. WHO, Vaccinations against Ebola begin in DR Congo City of Goma, *AlJAZEERA*, 22-07-2019. https://www.google.com/amp/s/www.aljazeera.com/amp/news/2019/07/vaccinations-ebola-dr-congo-city-goma-19071511221895.html.
18. WHO, WHO adapts Ebola Vaccination Strategy in the Democratic Republic of Congo to account for Insecurity and Community Feedback, 07-05-2019. https://www.who.int/news-room/detail/07-05-2019-who-adapts-ebola-vaccination-strategy-in-the-democratic-republic-of-congo-to-account-for-insecurity-and-community-feedback.
19. WHO, Public health round-up, *Bull. World Health* 97(12):793-794, 2019.
20. J. M. Hyman, J. Lie, E. A. Stanley, Modeling the Impact of Random Screening and Contact Tracing in Reducing the Spread of HIV, *Math. Biosci.* 181:17–54, 2003.
21. E. N. Bodine, C. Cook, M. Shorten, The Potential impact of a Prophylactic Vaccine for Ebola virus disease in Sierra Leone, *Math. Biosci.* 15:337–359, 2018.
22. J. C. Blackwood, L. M. Childs, The Role of Interconnectivity in Control of an Epidemic, *srep* 6:29263:1–10, 2016.
23. M. A. Safi, A. B. Gumel, Dynamics Analysis of a Quarantine Model in two Patches, *Math. Meth. Appl. Sci* 38:349–364, 2015.
24. A. Dénes, A. B. Gumel, Modeling the Impact of Quarantine During an Outbreak of Ebola Virus Disease, *Infect. Dis. Model.* 4:12–27, 2019.
25. M. Shen, Y. Xiao, L. Rong, Modeling the Effect of Comprehensive Interventions of Ebola Virus Transmission, *srep* 5.15818:1–14, 2015.
26. T. W. Tulu, B. Tian, Z. Wu, Modeling the Effect of Quarantine and Vaccination on Ebola Disease, *Adv. Differ. Equ* 2017:178:1–14, 2017.
27. M. L. Juga, F. Nyabadza, F. Chirove, Ebola Virus Disease with Fear and Environmental Transmission Dynamics, *Infect. dis. model.* 6:545–559, 2021.

28. A. Camacho, A. J. Kucharski, S. Funk, J. Breman, P. Piot, W. J. Edmunds, Potential for Large Outbreaks of Ebola Virus Disease, *Epidemics* 9:70–78, 2014.
29. K. Kabli, S. E. Moujaddid, K. Niri, A. Tridane, Comparative System Analysis of the Ebola Virus Epidemic Model, *Infect. dis. model.* 3:145–159, 2018.
30. Li Li, Transmission Dynamics of Ebola Virus Disease with Human Mobility in Sierra Leone, *Chaos Solitons Fractals* 104:575–579, 2017.
31. A. Rachah, D. F. M. Torres, Analysis, Simulation and Optimal Control of a SEIR Model for Ebola Virus with Demographic Effects, *Commun. Fac. Sci. Univ. Ank. Ser. A1 Math. Stat.* 67:179–197, 2018.
32. J-M. Zhu, L. Wang, J-B. Liu, Eradication of Ebola Based on Dynamic Programming, *Comput. Math. Methods Med.* 2016:1–9, 2016.
33. W. S. Hart, L. F. R. Hochfilzer, N. J. Cunniffe, H. L. N. Nishiura, R. N. Thompson, Accurate Forecasts of the Effectiveness of Interventions against Ebola may require Models that Account for Variations in Symptoms during Infection, *Epidemics* 29:1–10, 2019.
34. T. Berge, A. J. O. Tassé, H. M. Tenkam, Mathematical modeling of contact tracing as a control strategy of Ebola Virus Disease, *Int. J. Biomath.* 11:1850093–1–36, 2018.
35. C. E. Madubueze, A. R. Kimbir, T. Aboiyar, Global Model with Contact Tracing and Quarantine, *AppL. Appl. Math.* 13:382–403, 2018.
36. A. J. O. Tassé, B. Tsanou, J. Lubuma, J. L. Woukeng, Assessment of Effective Isolation-Safe burial and Vaccination Optimal Controls in an Ebola Epidemic Model, 2020. https://www.researchgate.net/publication/341953005_assessment_of _effective_isolation_safe_burial_and_vaccination_optimal_controls_in_an_Ebola_epidemic _model.
37. J. R. Glynn, H. Bower, S. Johnson, C. F. Houlihan, C. Montesano, J. T. Scott, M. G. Semple, M. Bangura, A. J. Kamara, O. Kamara, S. H. Mansaray, D. Sesay, C. Turay, S. Dicks, R. E. G. Wadoum, V. Colizzi, F. Checchi, D. Samuel, R. S. Tedder, Asymptomatic Infection and Unrecognised Ebola Virus Disease in Ebola-Affected Households in Sierra Leone: A Cross-Sectional Study Using a New Non-Invasive Assay for Antibodies to Ebola Virus, *Lancet Infect. Dis.* 17:645–53, 2017.
38. J. Legrand, R. F. Grais, P. Y. Boelle, A. J. Valleron, A. Flahault, Understanding the Dynamics of Ebola Epidemics, *Epidemiol. Infect.* 135:610–621, 2007.
39. E. M. Leroy et al., Human asymptomatic ebola infection and strong inflammatory response, *Lancet* 355:2210–2215, 2000.
40. M. O. Durojaye, I. J. Ajie, Mathematical Model of the Spread and Control of Ebola Virus Disease, *J. Appl. Math. Comput* 7:23–31, 2017.
41. A. Gideon, I. Miranda, Teboh-Ewungkem, A Mathematical Model with Quarantine states for the dynamics of Ebola Virus Disease in Human Populations, *Comput. Math. Methods Med.* 2016:1–29, 2016.
42. M.D. Ahmad, M. Usman,A. Khan, M. Imran, Optimal Control Analysis of Ebola disease with Control Strategies of Quarantine and Vaccination, *Infectious Diseases of Poverty* 5:72:1–12, 2016.
43. M. Imran, A. Khan, A. R. Ansari, Modeling Transmission Dynamics of Ebola Virus Disease, *Int. J. Biomath.* 10:1750057-1–35, 2017.
44. T. Berge, J. M. -S. Lubuma, G. M. Moremedi, N. Morris, R. Kondera-Shava, A Simple Mathematical Model for Ebola in Africa, *J. Biol. Dyn.* 11 (1):42–74, 2017.
45. Ebola Bodies are Infectious a Week After Death, Study Shows. https://time.com/3708994/ebola-bodies-infectious/.
46. WHO, Global Vaccine Safety. https://www.who.int/vaccine_safety /initiative/detection/immunization_misconception/ en/index2.html.

47. T. Berge, S. Bowong, J. M. -S.Lubuma, M. L. M. Manyombe, Modelling Ebola Virus Disease Transmissions with Reservoir in a Complex Virus Life Ecology, *Math. Biosci.* 15(1):21–56, 2018.
48. S. S. Nadim, I. Ghosh, J. Chattopadhyay, Short-Term Predictions and Prevention Strategies for COVID-2019: A Model Based Study, *Appl. Math. Comput.* 404:1–20, 2021.
49. F. B. Agusto, M. I. Teboh-Ewungkem, A. B. Gumel, Mathematical Assessment of the Effect of Traditionnal Beliefs and Customs on the Transmission Dynamics of the 2014 Ebola outbreaks, *BMC Medecine* 13:96:1–17, 2015.
50. T. Berge, M. Chapwanya, J. S. -M. Lubuma, Y. A. Terefe, A Mathematical Model for Ebola Epidemic with Self-Protection Measures, *J. Biol. Syst.* 11(1):42-74, 2016.
51. A. Brettin, R. Rossi-Goldthorpe, K. Weishaar, I. V. Erovenko, Ebola could be Eradicated through Voluntary Vaccination, *R. Soc. open sci* 5:171591:1–12, 2017.
52. North-Kivu, *Knoema*. https://knoema.com/atlas/Democratic-Republic-of-the -Congo/North-Kivu.
53. Sud-Kivu, *Knoema*. https://knoema.com/atlas/Democratic-Republic-of-the-Congo/Sud-Kivu.
54. A. Camacho, R. M. Eggo, S. Funk, C. H. Watson, A. J. Kucharski, Estimating the Probability of Demonstrating Vaccine Efficacy in the Declining Ebola Epidemic: A Bayesian Modelling Approach, *BMj Open* 5:e009346:1–6, 2015.
55. E. Grigorieva, E. Khailov, Determination of the Optimal Controls for an Ebola Epidemic Model, *Discrete Contin. Dyn. Syst. Ser. S* 11:1071–1101, 2018.
56. C. Yang, J. Wang, A Mathematical Model for the Novel Coronavirus Epidemic in Wuhan, China, *Math. Biosci. Eng.* 17(3):2708-2724, 2020.
57. J. Bartlett, J. Devinney, E. Pudlowski, Mathematical Modeling of the 2014/2015 Ebola Epidemic in West Africa, *SIAM J. Appl. Math.* 9:87–102, 2016.
58. P. Mbala-Kingebeni, C-J. Villabona-Arenas, N. Vidal, J. Likofata, J. Nsio-Mbeta, S. Makiala-Mandanda, D. Mukadi, P. Mukadi, C. Kumakamba, B. Djokolo, A. Ayouba, E. Delaporte, M. Peters, J-J. M. Tamfum, S. Ahuka-Mundeke, Rapid Confirmation of the Zaire Ebola Virus in the Outbreak of the Equateur Province in the Democratic Republic of Congo: Implications for Public Health Interventions, *Clin. Infect. Dis.* 68(2):330–333, 2019.
59. WHO, Liberia: Local Students Become Active Ebola Case Finders, 2014. https://www.who.int/features/2014/ebola-case-finding/en/.
60. K. A. Dautel, E. O. Agyingi, Modeling the Impact of Educational Campaign on the Transmission Dynamics of Ebola, *J. Biol. Syst.* 29:971–993, 2021.
61. B. Levy, C. Edholm, O. Gaoue, R. Kaondera-Shava, M. Kgosimore, S. Lenhart, B. Lephodisa, E. Lungu, T. Maarijani, F. Nyabadza, Modeling the Role of Public Health Education in Ebola Virus Disease Outbreaks in Sudan, *Inf. Dis. Model.* 2:323–340, 2017.
62. P. Chen, W. Fan, X. Guo, A Hybrid Simulation Model to Study the Impact of Combined Interventions on Ebola Epidemic, *Plos One* 16(7):e0254044, 2021.
63. J. M. Cénat, C. Rousseau, R. D. Dalexis, J. Bukaka, D. Derivois, O. Balayulu-Makila, J-P. Birangui, Knowledge and Misconceptions related to the Ebola Virus Disease among Adults in the Democratic Republic of theCongo: The Venomous Snake under Table of Prevention, *Public Health in Practice* 2:1–6, 2021.
64. G. O. Lawi, J. Y. T. Mugisha, N. Omolo-Ongati, Mathematical Model for Malaria and Meningitis Co-infection among Children, *Appl. Math. Sci.* 5:2337–2359, 2011.
65. C. Castillo-Chavez, B. Song, Dynamical Models of Tuberculosis and their Applications, *Math. Biosci. Eng.* 1(2):361–404, 2004.